International Journal of Heat and Mass Transfer 234 (2024) 126099

Contents lists available at ScienceDirect

International Journal of Heat and Mass Transfer

journal homepage: www.elsevier.com/locate/ijhmt

Development of new universal correlations for minimum heat flux point for saturated pool boiling of cryogens

Faraz Ahmad [a], Michael Meyer [b], Jason Hartwig [c], Issam Mudawar [a,b,*,1]

[a] Purdue University Boiling and Two-Phase Flow Laboratory (PU-BTPFL), School of Mechanical Engineering, 585 Purdue Mall, West Lafayette, IN 47907, USA
[b] MTS Inc., 3495 Kent Ave, West Lafayette, IN 47906, USA
[c] NASA Glenn Research Center, Fluids and Cryogenics Branch, Cleveland, OH 44135, USA

ARTICLE INFO

Keywords:
Minimum heat flux
Pool boiling
Saturated conditions
Cryogens
Correlations

ABSTRACT

This study addresses the critical need for a reliable database for the minimum heat flux (MHF) point in saturated pool boiling of cryogens. Relying on a comprehensive review of the relatively sparse published literature, a key objective of the study is to amass a MHF database, which is then used to investigate influences of various parameters on MHF, assess the accuracy of published correlations, and develop new correlations specifically tailored to cryogenic fluids. By applying stringent point-by-point evaluation criteria, 165 data points for MHF point temperature (T_{min}) and 158 data points for MHF point heat flux (q''_{min}) are aggregated, comprising this study's "Consolidated Database" for MHF. This database includes data for liquid helium (LHe), liquid argon (LAr), liquid hydrogen (LH_2), and liquid nitrogen (LN_2) and boiling from clean as well as treated (coated or oxidized) surfaces. A total of 9 correlations for T_{min} and 10 for q''_{min} are evaluated for accuracy against the new Consolidated Database. Leveraging insights from prior correlation results and trends from the new Consolidated Database, new universal correlations are formulated for both T_{min} and q''_{min}. The new correlation for T_{min} features Mean Absolute Errors (MAEs) of 9.05 % for clean surfaces and 7.7 % for treated surfaces. Similarly, the new q''_{min} correlation shows MAEs of 21.50 % for clean surfaces and 25.22 % for treated surfaces. While the new correlations represent a significant advancement in the development of predictive tools for cryogens, this study points to a need for more comprehensive experimental investigation of heat transfer aspects of cryogens, which will undoubtedly further improve the robustness and accuracy of the new correlations.

1. Introduction

1.1. Cryogens and their applications

The term "cryo" refers to extreme "cold" or "frost" and the science dealing with such extremely low temperatures and its application is called cryogenics. Cryogenic fluids are a unique class of substances characterized by extremely low saturation temperatures, which set them apart from common fluids like water and refrigerants. This distinction is visually depicted in Fig. 1, wherein REFPROP 10 [1] is used to establish the saturation temperatures of the different fluids. Furthermore, a comprehensive comparative analysis conducted by Ganesan et al. [2] across different coolant classes has revealed significant disparities in several properties of saturated liquids. They include liquid density (ρ_f), specific heat of liquid at constant pressure ($c_{p,f}$), liquid thermal conductivity (k_f), liquid viscosity (μ_f), liquid Prandtl number (Pr_f). Aside from the cryogens having low values of μ_f, they also feature low values of vapor density (ρ_g), latent heat of vaporization (h_{fg}), and surface tension (σ), but elevated values of specific heat of vapor ($c_{p,f}$). These unique thermophysical attributes distinguish cryogenic fluids, especially liquid helium (LHe), from conventional fluids. This underscores the distinct transport characteristics of cryogens as well as the difficulty predicting these characteristics using predictive methods developed for common fluids.

The unique physics of cryogens helps explain their broad range of applications in important and often challenging environments. For instance, cryogens find extensive use in the medical field, where they are employed to generate extremely low temperatures for various purposes, including tissue freezing, storing of reproductive cells, and preservation of biological samples. Cryogens also play a crucial role in the development and operation of superconductors, many of which can only

* Corresponding author.
E-mail address: mudawar@ecn.purdue.edu (I. Mudawar).
[1] https://engineering.purdue.edu/BTPFL

https://doi.org/10.1016/j.ijheatmasstransfer.2024.126099
Received 17 May 2024; Received in revised form 12 July 2024; Accepted 19 August 2024
Available online 24 August 2024

Nomenclature

A	atomic number
c_p	specific heat at constant pressure [J. kg^{-1}. K^{-1}]
g	gravitational acceleration [m. s^{-2}]
h_{fg}	latent heat of vaporization [J. kg^{-1}]
k_w	thermal conductivity of heated surface [W. m^{-1}. K^{-1}]
k_c	thermal conductivity of coated material [W. m^{-1}. K^{-1}]
L_b	bubble length scale [m], $L_b = \left[\frac{\sigma}{g(\rho_f-\rho_g)}\right]^{\frac{1}{2}}$
N	number of data points
Nu_g	Nusselt number for vapor; $Nu_g = \frac{hL_b}{k_g}$
p	pressure [N. m^{-2}]
p^*	reduced pressure; $p^* = p/p_c$
p_c	critical pressure [N. m^{-2}]
Pr	Prandtl number
q''	heat flux per unit surface area [W. m^{-2}]
q''_{min}	minimum heat flux [W. m^{-2}]
R_g	Specific gas constant [J. kg^{-1}. K^{-1}]
S_q	surface characteristics multiplier for new minimum heat flux correlation
S_T	surface characteristics multiplier for new minimum temperature correlation
T	temperature [K]
T_c	critical temperature [K]
T_{min}	minimum film boiling temperature [K]
T_{sat}	saturation temperature [K]
ΔT_{sat}	wall superheat, $T_w - T_{sat}$ [K]
T_w	heated wall temperature [K]
v	specific volume [m^3. kg^{-1}]

Greek symbols

α	percentage of predictions within ±30% of the data
β	percentage of predictions within ±50% of the data
δ	thickness of surface coating [m]
θ	orientation angle of heated surface [°]
λ	wavelength [m]
μ	dynamic viscosity [Pa. s]
ρ	density [kg. m^{-3}]
σ	surface tension [N. m^{-1}]

Subscripts

c	critical point
exp	experimental (measured)
f	saturated liquid
g	saturated vapor
min	minimum
$pred$	predicted (calculated)
sat	saturation
w	heating wall

Acronyms

CHF	critical heat flux
HTC	heat transfer coefficient
MHF	minimum heat flux
LAr	liquid argon
LCH_4	liquid methane
LH_2	liquid hydrogen
LHe	liquid helium
LN_2	liquid nitrogen
LO_2	liquid oxygen
MAE	mean absolute error
NASA	National Aeronautics and Space Administration
ONB	onset of nucleate boiling
PU-BTPFL	Purdue University Boiling and Two-Phase Flow Laboratory

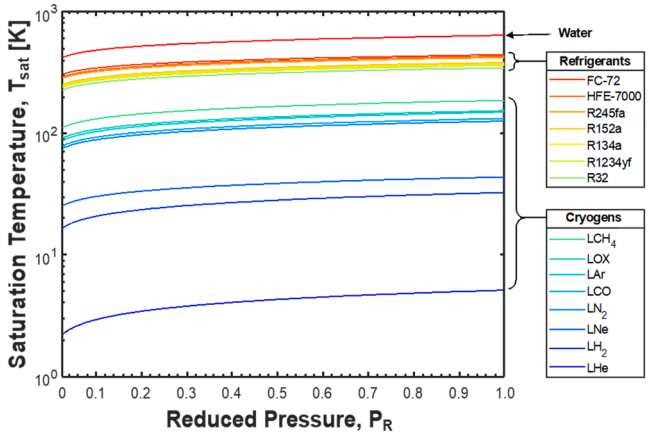

Fig. 1. Classification of coolants into water, refrigerants, and cryogens based on variation of saturation temperature with reduced pressure.

function at cryogenic temperatures, which highlights the indispensable role of cryogens in this area. And the exceptional energy density of cryogens such as liquid oxygen (LO_2) and liquid hydrogen (LH_2) render them ideal choices in rocket fuels for space exploration missions. Their properties enable spacecraft to achieve high thrust and energy efficiency; both are crucial for long-distance missions. In summary, the versatility and unique transport characteristics of cryogens renders them indispensable across a wide range of disciplines and applications.

1.2. Background physics of pool boiling

Pool boiling is a simple and effective method for efficient two-phase cooling. It is widely used across both low-temperature and high-temperature cooling applications. Examples of the low-temperature applications include cooling of electronic and power devices and superconductor coils. These applications leverage the high latent heat capacity of a coolant to efficiently dissipate large amounts of heat while maintaining relatively low, safe surface temperatures. On the other hand, in high-temperature applications, pool boiling is commonly used to quench metal alloy parts during heat treating processes in pursuit of superior mechanical properties.

Researchers use the boiling curve to understand the different phases of pool boiling, derived via one of two methods: steady-state heating and transient cooling (quenching). The steady-state method is preferred for its more accurate heat transfer measurements, which aids the comprehensive understanding of pool boiling mechanisms.

Fig. 2(a) shows a boiling curve constructed using the steady-state heating method, which is conducted in two separate phases. The first phase involves gradually increasing the wall heat flux from zero in small steps and recording wall temperature after reaching steady state. This allows capture of several key regions and transition points of pool boiling: single-phase liquid region, onset of nucleate boiling (ONB) point, nucleate boiling region, critical heat flux (CHF) point, and upper portion of the film boiling region. The second phase involves decreasing the heat flux in small steps starting in film boiling. This allows capture of the lower portion of the film boiling region, minimum heat flux (MHF) point, nucleate boiling region, and eventually the single-phase liquid

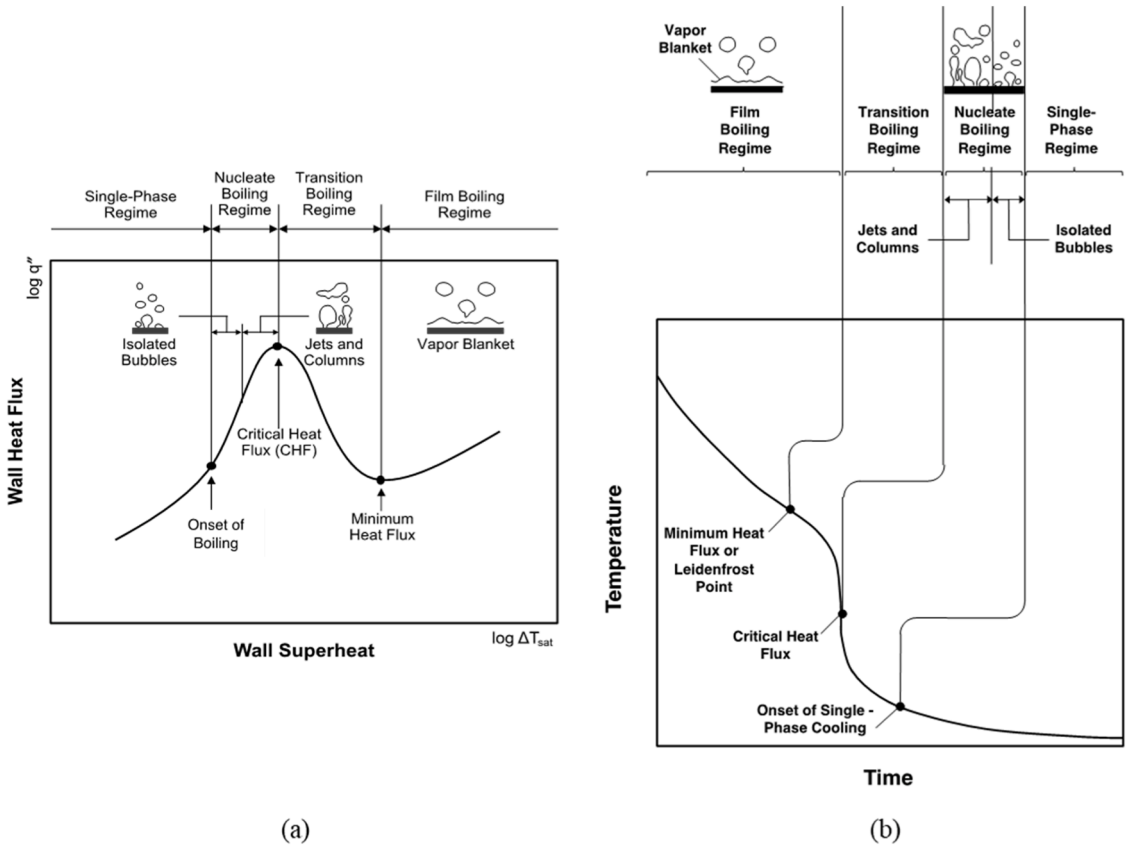

Fig. 2. (a) Pool boiling curve, generally measured using the steady-state heating method. (b) Pool quench curve, generally measured using the transient (quench) method.

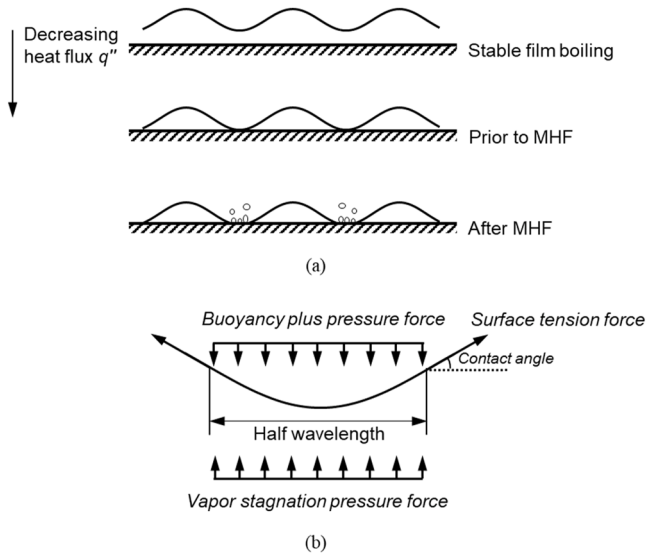

Fig. 3. (a) Schematic representation of initiation of the MHF condition by decreasing heat flux from film boiling. (b) Force balance for the half wavelength trough region of a unit interface cell.

region. However, lacking in the heating method is ability to capture the transition boiling region.

Fig. 2(b) shows the temperature-time cooling curve acquired using the alternative quenching method. Here, the surface is initially pre-heated to an elevated temperature well within the film boiling region, which is followed by transient cooling (quenching), which allows capture of all the boiling regions, including transition boiling, as well as all transition points of the boiling curve. Unlike the heating method, the corresponding boiling curve using the quenching method is highly dependent on the wall thermal mass and requires use of the lumped capacitance method to determine the relationship between wall heat flux and wall temperature across each boiling region.

The present study is in systematic continuation of efforts at the Purdue University Boiling and Two-Phase Flow Laboratory (PU-BTPFL) dating back to the mid-1980s and encompassing boiling characteristics of virtually every type of boiling configuration or scheme: capillary [3], pool [4], falling film [5], macro-channel [6], micro-channel [7], jet [8], and spray [9], as well as hybrid methods combining two or more schemes [10,11]. These studies involve the use of advanced experimental methods to acquire comprehensive databases, construct high-accuracy empirical correlations, as well as develop theoretical, computational, and machine learning models. Boiling of cryogenic fluids constitutes a major but relatively recent thrust for PU-BTPFL whose aim is to develop reliable predictive methods for cryogens like those developed earlier for common coolants.

1.3. Minimum heat flux (MHF) point

In the stable film boiling phase depicted in Fig. 3, a continuous vapor film acts to thermally insulate the heating surface. As the wall heat flux is decreased towards the MHF point, liquid gradually approaches the heating surface but without making direct contact. Further reduction in heat flux eventually leads to the MHF condition, when the combined downward buoyancy force (caused by the heavier liquid residing above the lighter vapor) and pressure force (induced by interfacial curvature), which push the interface towards the surface, just surpass the combined upward surface tension force and stagnation pressure force of newly

Table 1
Prior models and correlations for MHF temperature (T_{min}).

No.	Year	Author(s)	Correlations	Remarks
1	1961	Berenson [28]	$T_{min} = T_{sat} + 0.127\frac{\rho_g h_{fg}}{k_g}\left[\frac{g(\rho_f-\rho_g)}{\rho_f+\rho_g}\right]^{\frac{2}{3}}\left[\frac{\sigma}{g(\rho_f-\rho_g)}\right]^{\frac{1}{2}}\left[\frac{\mu_f}{(\rho_f-\rho_g)}\right]^{\frac{1}{3}}$	• First author to calculate Tmin by using his q"min correlation • Adopts Taylor instability to model the vapor film thickness
2	1963	Spiegler et al. [27]	$T_{min} = \frac{27}{32}T_c$	• Simplest correlation in the literature based exclusively on T_c. • This formulation was criticized by other researchers for failing to account for pressure effects
3	1973	Baumeister & Simon [29]	$T_{min} = \frac{27}{32}\,T_c\left\{1-\exp\left(-0.52\left[\frac{10^4\left(\frac{\rho_s}{A}\right)^{\frac{4}{3}}}{\sigma}\right]^{1/3}\right)\right\}$	• Uses concept of surface energy to account for heating surface effects • First to account for the solid surface effects
4	1974	Henry [30]	$T_{min} = T_{min,\,B} + 0.42\left(T_{min,\,B} - T_f\right)\left(\frac{k_f\rho_f c_{p,}}{k_w\rho_w c_{p,w}}\right)^{\frac{3}{10}}\left[\frac{h_{fg}}{c_{p,w}\left(T_{min,\,B}-T_f\right)}\right]^{\frac{3}{5}}$ where $T_{min,B}$ is T_{min} based on Berenson's correlation [28]	• Author mentions that Berenson's correlation underestimates the value of T_{min} because of failure to account for surface-fluid interaction • Incorporated properties of both solid and fluid
5	1975	Kalinin et al. [31]	$T_{min} = T_{sat} + (T_c - T_{sat})\left[0.16 + 2.4\left(\frac{k_f\rho_f c_{p,f}}{k_w\rho_w c_{p,w}}\right)^{\frac{1}{4}}\right]$	• Accounts for effects of both pressure and wall properties • One of the most accurate correlations in literature • Validated for cryogens
6	1976	Lienhard [32]	$T_{min} = T_{sat} + T_c\left(0.905 - \left(\frac{T_{sat}}{T_c}\right) + 0.095\left(\frac{T_{sat}}{T_c}\right)^8\right)$	• Utilizes Van der Waals' equation along with Maxwell's criteria for correlation development
7	1984	Sakurai et al. [13]	For 3-mm diameter heating surface: $T_{min} = 480 + 9e^{1.92p},\ p \le 1.1\ MPa$ $T_{min} = 480 + 80e^{0.27(p-1.1)},\ p > 1.1\ MPa$ For 1.2 mm and 2 mm diameter heaters: $T_{min} = 480 + 10e^{(2.2p)},\ p \le 0.94\ MPa$ $T_{min} = 480 + 80e^{0.34(p-0.94)},\ p > 0.94\ MPa$	• Developed for water and inapplicable to other fluids • Entirely empirical and not based on any physical mechanism
8	1990	Schroeder-Richter & Bartsch [33]	$h_g(T_g) - h_f(T_{min}) = 0.5\left[v_g(T_g) - v_f(T_{min})\right]\left[p_{sat}(T_{min}) - p_{sat}(T_g)\right]$	• Utilizes Clausius-Clapeyron equation • Implicit formulation compromises adoption of this correlation
9	2018	Aursand et al. [34]	$T_{min} = \frac{1}{3}T_{sat} + \frac{2}{3}T_{sat}\left[1+\frac{9\sigma}{4+\frac{\mu_f}{\mu_g}}\frac{\sqrt{2\pi R_g T_{sat}}}{k_g f(\varepsilon)}\right]^{\frac{1}{2}}$ where $f(\varepsilon)$ is a function of evaporation coefficient ε	• Uses thermocapillary instability in the correlation's formulation • Difficult to use due to use of unknown evaporation effect function $f(\varepsilon)$
10	2021	Cai et al. [12]	$T_{min} = T_{sat} + 0.1223\left(\frac{\rho_f}{\rho_g}\right)^{-0.2029}\frac{\rho_g h_{fg}}{Nu_g k_g}\left[\frac{\sigma^3}{g\rho_g^2(\rho_f-\rho_g)}\right]^{\frac{1}{4}}$	• Based on Cai et al.'s $q"_{min}$ correlation [12], which is combined with Klimenko's [42] Nusselt number correlation

formed vapor beneath, which tend to lift the interface away from the surface. This causes the liquid-vapor interface to contact and wet the surface, leading to intense boiling and vapor production in the wave trough. By examining the interface's half wavelength trough region, Cai et al. [12] suggested the MHF condition occurs when these four forces reach equilibrium.

1.4. Parameters influencing MHF point

MHF plays a significant role in pool boiling because it marks significant changes in heat transfer effectiveness between the inefficient film boiling and more efficient transition boiling. Extensive research has been conducted to explore the various factors influencing MHF, including system pressure, surface material, surface treatment, and surface orientation, contributing to a mechanistic understanding of this important phenomenon.

For instance, Sakurai et al. [13] examined the impact of *system pressure* on both MHF point surface temperature, T_{min}, and MHF point heat flux, $q"_{min}$, for water across a broad pressure range from 20 kPa to 2 MPa. They reported the values of both MHF parameters increased monotonically with increasing pressure. However, while these increases were appreciable at lower pressures (<1.1 MPa), they were far less so at higher pressures (>1.1 MPa). The weaker changes at high pressures suggested the experimental results do not align with theoretical formulations of MHF based on the Taylor instability. Kozlove et al. [14] conducted experiments with LH_2 on three different surfaces: copper, aluminum, and stainless steel, over a pressure range of 7.2–130 kPa. Their findings aligned with those of Sakurai et al. [13], namely that values of both T_{min} and $q"_{min}$ increase with increasing pressure. In contrast, Deev et al. [15], who conducted experiments with LHe over relatively high pressures corresponding to reduced pressures of $p^* = 0.445–0.98$, found a monotonic decreases in both T_{min} and $q"_{min}$ with increasing pressure; they also reported similar trends for the CHF point, where both T_{CHF} and $q"_{CHF}$ also deceased with increasing pressure. Similar MHF trends were reported for LHe by other investigators [16–19]. At first glance, these findings may seem contradictory to those from studies involving other cryogens. However, upon closer examination, it becomes evident that the impact of pressure on T_{min} and $q"_{min}$ is multifaceted and varies across different pressure ranges. Specifically, for lower pressures, increasing system pressure increases the values of both T_{min} and $q"_{min}$. However, this positive trend is either slowed significantly or reversed altogether at higher pressures.

Another factor influencing boiling phenomena in general is *surface material*, a facet that has not received sufficient systematic investigation in previous MHF literature. Nonetheless, there are a few noteworthy studies that provide evidence of this influence. For instance, Grigoriev et al. [20] compared the boiling characteristics of LHe on copper and stainless steel surfaces and reported that stainless steel exhibited higher values of both T_{min} and $q"_{min}$. Furthermore, they noted that stainless steel transitioned directly from nucleate boiling to film boiling, bypassing the transition boiling region. This behavior of stainless steel was attributed to its inferior thermophysical properties, particularly thermal conductivity. Similar experiments by Kozlov et al. [14] corroborated these findings by comparing MHF results for copper, aluminum, and stainless steel. They too reported that increasing the thermal conductivity of the heating surface decreases the values of both T_{min} and $q"_{min}$. In general, changing the solid-fluid combination is expected to always influence boiling behavior.

Table 2
Prior models and correlations for minimum heat flux (q''_{min}).

No.	Year	Author(s)	Correlations	Remarks
1	1959	Kutateladze [35]	$q''_{min} = C\, h_{fg}\left(g\rho_g^2\frac{\rho_f+\rho_g}{\rho_f}\right)^{\frac{1}{2}}\left[\frac{\sigma(\rho_f-\rho_g)}{\rho_g}\right]^{\frac{1}{4}}$ where C is an empirical constant	• Pioneering work for q''_{min} • Uses equations of motion to develop the correlation
2	1959	Zuber [36]	$q''_{min} = 0.17658\,\rho_g h_{fg}\left[\frac{\sigma g(\rho_f-\rho_g)}{(\rho_f+\rho_g)^2}\right]^{\frac{1}{4}}$	• Another pioneering work for q''_{min} • Utilizes Rayleigh-Taylor instability to derive the correlation
3	1961	Berenson [28]	$q''_{min} = 0.09\,\rho_g h_{fg}\left[\frac{g(\rho_f-\rho_g)}{\rho_f+\rho_g}\right]^{\frac{1}{2}}\left[\frac{\sigma}{g(\rho_f-\rho_g)}\right]^{\frac{1}{4}}$	• *Utilizes Taylor-Helmholtz instability to formulate the q''_{min} correlation, which then used develop the develop correlation for T_{min}* • *Based on hypothesis that the heat is transferred across a thin vapor layer via conduction* • Based on dimensional analysis
4	1962	Morozov [37]	$q''_{min} = 0.0267\,\rho_g h_{fg}\left[\frac{\sigma g(\rho_f-\rho_g)}{\rho_g^2}\right]^{\frac{1}{4}}$	
5	1966	Padilla [38]	$q''_{min} = 0.14\,\rho_g h_{fg}\left[\frac{\sigma g(\rho_f-\rho_g)}{(\rho_f+\rho_g)^2}\right]^{\frac{1}{4}}$	• Based on Zuber's [36] formulation • Adjusts coefficient value based on data for film boiling of potassium on horizontal stainless-steel surface
6	1967	Kesselring et al. [39]	$q''_{min} = 0.1282\,\rho_g h_{fg}\frac{\sigma g(\rho_f-\rho_g)}{(\rho_f+\rho_g)^2}$	• Developed for strips • Shows q''_{min} depends on strip width for widths smaller than 2 times dangerous wavelength
7	1975	Kalinin et al. [31]	$q''_{min} = 0.18\,\Delta T_{min}\left[\frac{c_{p,g}k_g^2}{\mu_g}\rho_g g(\rho_f-\rho_g)\right]^{\frac{1}{3}}$ where $\Delta T_{min} = (T_c - T_{sat})\left[0.16 + 2.4\left(\frac{k_f\rho_f c_{p,f}}{k_w\rho_w c_{p,w}}\right)^{\frac{1}{4}}\right]$	• First correlation for T_{min} which accounts for solid-fluid contact • T_{min} correlation is used to derive the q''_{min} correlation • Accounts for effects of wall properties, rendering it more superior than most other correlations
8	1980	Lienhard & Dhir [40]	$q''_{min} = 0.091\,\rho_g h_{fg}\left[\frac{\sigma g(\rho_f-\rho_g)}{(\rho_f+\rho_g)^2}\right]^{\frac{1}{4}}$	• Based on assumptions very similar to Zuber's [36] • Assumes MHF point is outcome of the collapse of the vapor film
9	1987	Shoji & Nagano [41]	For $\frac{\rho_g}{\rho_f} > 0.005 : q''_{min} =$ $0.00189\,\rho_g h_{fg}\left(\frac{\rho_g}{\rho_f}\right)^{-0.73}\left[\frac{\sigma g(\rho_f-\rho_g)}{(\rho_f+\rho_g)^2}\right]^{\frac{1}{4}}$ For $\frac{\rho_g}{\rho_f} < 0.005 : q''_{min} =$ $0.0212\,\rho_g h_{fg}\left(\frac{\rho_g}{\rho_f}\right)^{-0.26}\left[\frac{\sigma g(\rho_f-\rho_g)}{(\rho_f+\rho_g)^2}\right]^{\frac{1}{4}}$	• Uses Zuber's formulation [36] as base • Incorporates density ratio effects • Different correlations recommended for different ranges of density ratio
10	2021	Cai et al. [12]	$q''_{min} = 0.01947\left(\frac{\rho_f}{\rho_g}\right)^{-0.2029}\rho_g h_{fg}\left[\frac{\sigma g(\rho_f-\rho_g)}{\rho_g^2}\right]^{\frac{1}{4}}$	• Formulation based on force balance on a unit cell of the wavy liquid-vapor interface over a flat horizontal surface • Based on hypothesis that the interface is dominated by the Taylor instability, wherein the distance between two wave peaks equals the critical Taylor wavelength and any wave exceeding this wavelength would lead to vapor rupture

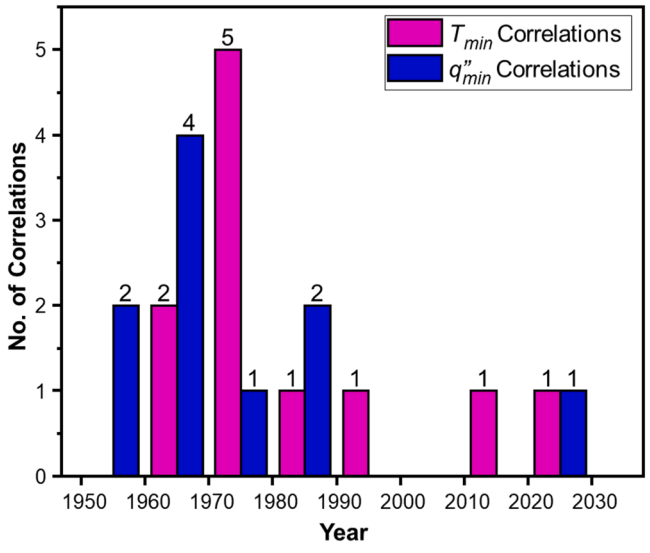

Fig. 4. Number of correlations published per decade.

Moving beyond surface material, based on findings from numerous past investigations, *surface treatment* emerges as another parameter that can significantly influence T_{min} and q''_{min}. For example, Butler et al. [17] conducted experiments with LHe to investigate the influence of surface treatment on heat transfer characteristics on a copper surface in superconducting magnet applications. They reported surface treatment via coating increased both T_{min} and q''_{min} (also q''_{CHF}), with q''_{min} being fourfold higher for a treated surface compared to a plain copper surface. Ogata and Mori [21] investigated the influence of coating a copper surface with epoxy resin on boiling behavior of LHe. They showed that increasing the thickness of coating increased the values of both T_{min} and q''_{min}. Chandratilleke et al. [22] confirmed these trends for LHe but also examined the effect of thermal conductivity of coating material, increasing which was shown to decrease the values of both T_{min} and q''_{min}. They further found that the effect of thickness of coating material is more pronounced with an insulating Teflon coating compared to a stainless steel (SUS 304) coating. Similar to the surface coating, oxidizing the heated surface was shown by Iwamoto et al. [23] to also increase values of both T_{min} and q''_{min} for LHe.

Orientation of the heating surface is yet another parameter whose impact on the MHF point has received attention in prior literature. Iwamoto et al. [23] investigated this effect for LHe across orientation angles ranging from horizontal upward-facing ($\theta = 0°$) to horizontal downward-facing ($\theta = 180°$). They reported a weak impact on q''_{min} despite a slight increase from $\theta = 0°$ to 90° followed by a slight decrease

Table 3
Summary of number of cryogenic MHF datapoints acquired from published sources and those excluded from consideration, along with reasons for the exclusions.

No.	Year	Author(s)	No. of Acquired Datapoints	No. of Excluded Datapoints	Reasons for Data Exclusion
1	1960	Class et al. [44]	17	17	• These points were determined to be the lowest points of the film boiling region and not MHF points
2	1965	Wayner & Bankoff [45]	3	3	• Porous plate data
2	1966	Cummings & Smith [46]	1	0	
3	1967	Clark et al. [47]	7	0	
4	1969	Price [48]	6	6	• These points were determined to be the lowest points of the film boiling region and not MHF points
4	1969	Buttler et al. [17]	2	0	
5	1970	Merte [49]	22	6	• Duplicate data
6	1972	Sauer & Ragsdell [50]	5	5	• MHF point was not clearly mentioned
7	1974	Jergel and Stevenson [51]	3	0	
7	1975	Swanson & Bowman [52]	1	0	
8	1977	Deev et al. [15]	32	0	
9	1977	Grigoriev et al. [20]	2	0	
10	1977	Ogata & Nakayama [53]	3	0	
11	1981	Ogata [54]	1	0	
12	1982	Kleminko & Shelepen [55]	3	1	• MHF point was not clearly mentioned
13	1982	Schiewe & Hartmann [56]	4	0	
14	1986	Nishio [57]	2	0	
15	1989	Chandratilleke et al. [22]	16	0	
16	1989	Nishio & Chandratilleke [58]	1	0	
17	1992	Kozlov & Nozdrin [14]	11	1	• T_{min} value was not given in the table
18	1993	Ogata & Mori [21]	9	0	
19	1994	Iwamoto et al. [59]	12	8	• 2- and 3-mm channels under heated plate: in two-thirds of the experimental results, the boiling surface had cooling channels to investigate their influence on MHF and CHF
20	1996	Iwamoto et al. [23]	24	0	
21	1998	Iwamoto et al. [60]	24	0	
22	2009	Jin et al. [61]	1	0	
Total			**209**	**44**	

until $\theta = 180°$. Similarly, Chandratilleke et al. [22] found that T_{min} for LHe was rather unaffected by surface orientation angle.

1.5. Inferences drawn from literature review

Based on the authors' review of prior literature, several crucial insights and inferences can be drawn regarding parametric trends of MHF:

1. Different trends regarding the effects of system pressure on T_{min} and $q"_{min}$ have been reported. However, upon closer examination, it becomes evident that the impact of pressure on MHF parameters is multifaceted and varies across different pressure ranges. Specifically, for lower pressures, increasing system pressure increases the values of both T_{min} and $q"_{min}$. However, this trend diminishes and even reverses at high pressures. This underscores the need for a more thorough investigation of system pressure effects over the entire pressure range for multiple cryogens.
2. Previous investigators have consistently reported that increasing the thermal conductivity of the heating surface has a positive impact on heat transfer effectiveness across different boiling regions. Increasing the thermal conductivity has also been show to decrease values of both T_{min} and $q"_{min}$.
3. Prior studies indicate that surface treatments and coatings do not affect the heat transfer coefficient within film boiling, where the surface is shielded from liquid contact via a continuous insulating vapor layer. However, as discussed later, our analysis does show that coatings and surface oxidation do increase values of both T_{min} and $q"_{min}$. This is especially the case for thicker and non-metallic coatings.
4. Published works point to surface orientation having significant influence on heat transfer effectiveness in certain boiling regions, especially at CHF and within film boiling, while the impact on T_{min} and $q"_{min}$ is comparatively small.

1.6. Objectives of the present study

The present study constitutes a crucial part of a U.S. initiative aimed at developing predictive tools for design and thermal performance assessment of cryogenic systems employed in space exploration missions, including fuel storage, transfer, and utilization. Particular emphasis is being placed on supporting the objectives of in-situ resource utilization (ISRU) as outlined by the National Aeronautics and Space Administration (NASA), encompassing a wide range of applications, scales, and environments relevant to upcoming missions to the Moon and Mars. The ongoing studies at PU-BTPFL aim collectively to develop new heat transfer correlations for each segment and transition point of the boiling curve for cryogens. The present work is a follow-up to recent joint studies by PU-BTPFL and NASA's Glenn Research Center, which were centered on prediction of pool boiling CHF [24], nucleate boiling heat transfer coefficient (HTC) [25], and film boiling HTC [26] for cryogens.

The present study will delve into developing similar predictive correlations for MHF in terms of both T_{min} and $q"_{min}$. This targeted analysis encompasses saturated pool boiling from flat surfaces with surface orientations ranging from horizontal upward-facing to horizontal downward-facing. The key objectives of the study can be summarized as follows:

Table 4
Summary of consolidated database.

Reference	Acceptable datapoints	Heater geometry	Heater size: Width x Length [mm^2] or diameter (Thickness) [mm]	Heater material	Surface condition	Pressure [MPa]	Inclination angle	Boiling state
LN_2								
Clark et al. (1967) [47]	7	Circular	76.2, (20.64)	Copper	Clean	0.097-0.5	0°, 90°, 180°	Saturated
Swanson & Bowman (1975) [52]	1	Circular	12.7 (not mentioned)	Copper	Clean	0.10133	0°	Saturated
Nishio (1986) [57]	2	Circular	22 (170)	Copper	Clean	0.10133	0°	Saturated
Merte (1970) [49]	11	Circular	76.2, (20.64)	Copper	Clean	0.0986	0°, 90°, 180°	Saturated
Kleminko & Shelepen (1982) [55]	1	Circular	40 (20)	Copper	Clean	0.10133	0°	Saturated
Schiewe & Hartmann (1982) [56]	4	Rectangular	-	Copper	Clean	0.10133	0°, 90°	Saturated
Jin *et al.* (2009) [61]	1	Square	60 × 60 (17.5)	Stainless steel	Clean	0.1	0°	Saturated
	27 acceptable datapoints for LN_2							
LHe								
Cummings & Smith (1966) [46]	1	Circular	15.24 (50)	Copper	Clean	0.10133	0°	Saturated
Butler et al. (1969) [17]	2	Rectangular	10 × 50 (5)	Copper	Clean	0.10133	0°	Saturated
Gergel (1974)	3	Circular	15 (10)	Al 69	Clean	0.10133	0°, 90°, 180°	Saturated
Grigoriev *et al.* (1977) [20]	2	Circular	8 (40)	Copper M-1, stainless steel X18H9T	Clean	0.10133	0°	Saturated
Deev *et al.* (1977) [15]	32	Square	30 × 30	Copper (99.993%)	Clean	0.103 – 0.22	0°, 90°	Saturated
Ogata & Nakayama (1977) [53]	3	Square, Circular	15 × 15, 6.1	Copper	Clean	0.10133	0°	Saturated
Ogata et al. (1981) [54]	1	Square	15 × 15	Copper	Clean	0.10133	0°	Saturated
Chandratilleke et al. (1989) [22]	16	Circular	20 (30)	Copper	Polished, PTFE coating, SUS 304 coating	0.10133	0°, 90°, 175°	Saturated
Nishio & Chandratilleke (1989) [58]	1	Circular	20 (30)	Copper	Clean	0.10133	90°	Saturated
Ogata et al. (1993) [75]	9	Square	15 × 15 (8)	Copper	Clean, Coated	0.10133	0°, 90°	Saturated
Iwamoto et al. (1994) [59]	4	Rectangular	76 × 18 (7.5)	Copper	Clean	0.10133	0°, 30°, 90°, 165°	Saturated
Iwamoto et al. (1996) [23]	24	Rectangular	76 × 18 (7.5)	Copper	Polished, oxidized	0.10133	0°, 30°, 90°, 165°	Saturated
Iwamoto *et al.* (1998) [60]	24	Rectangular	18 × 10 (7.5), 18 × 18 (7.5), 18 × 40 (7.5), 18 × 76 (7.5)	Copper	Clean	0.1013	0°, 90°	Saturated
	122 acceptable datapoints for LHe							
LH_2								
Merte (1970) [49]	6	Circular	76.2	Copper	Clean	0.1023 – 0.1027	0°, 90°, 180°	Saturated
Kozlov & Nozdrin (1992) [14]	9	Circular	30 (8, 18, 12)	Stainless steel, aluminum alloy, copper	Clean	0.016 – 0.13	0°	Saturated
	15 acceptable datapoints for LH_2							
LAr								
Kleminko & Shelepen (1982) [55]	1	Disk	40 (20)	Copper	Not mentioned	0.10133	0°	Saturated
	1 acceptable datapoint for LAr							
	165 acceptable data points for all four cryogens							

i. Conduct an exhaustive literature survey to identify all factors influencing MHF.
ii. Compile previously published correlations for both T_{min} and q''_{min}.
iii. Collect and organize MHF data from literature sources available across the globe.
iv. Examine the amassed data on a point-by-point basis, and apply systematic data exclusion criteria to culminate in a new Consolidated Database encompassing LHe, LH_2, LN_2, and LAr, cryogens for which MHF data are available
v. Assess the predictive performance of all gathered correlations against the Consolidated Database.
vi. Synthesize the findings from the literature review with the insights gained from the evaluation of existing correlations and parametric trends of the Consolidated Database to construct new correlations for T_{min} and q''_{min} for cryogens that outperform the prior correlations.

2. Review of prior models and correlations for MHF point

In contrast to the considerable attention given to nucleate boiling, film boiling, and CHF, studies addressing MHF are relatively sparse. One possible explanation for this disparity is limited understanding of the

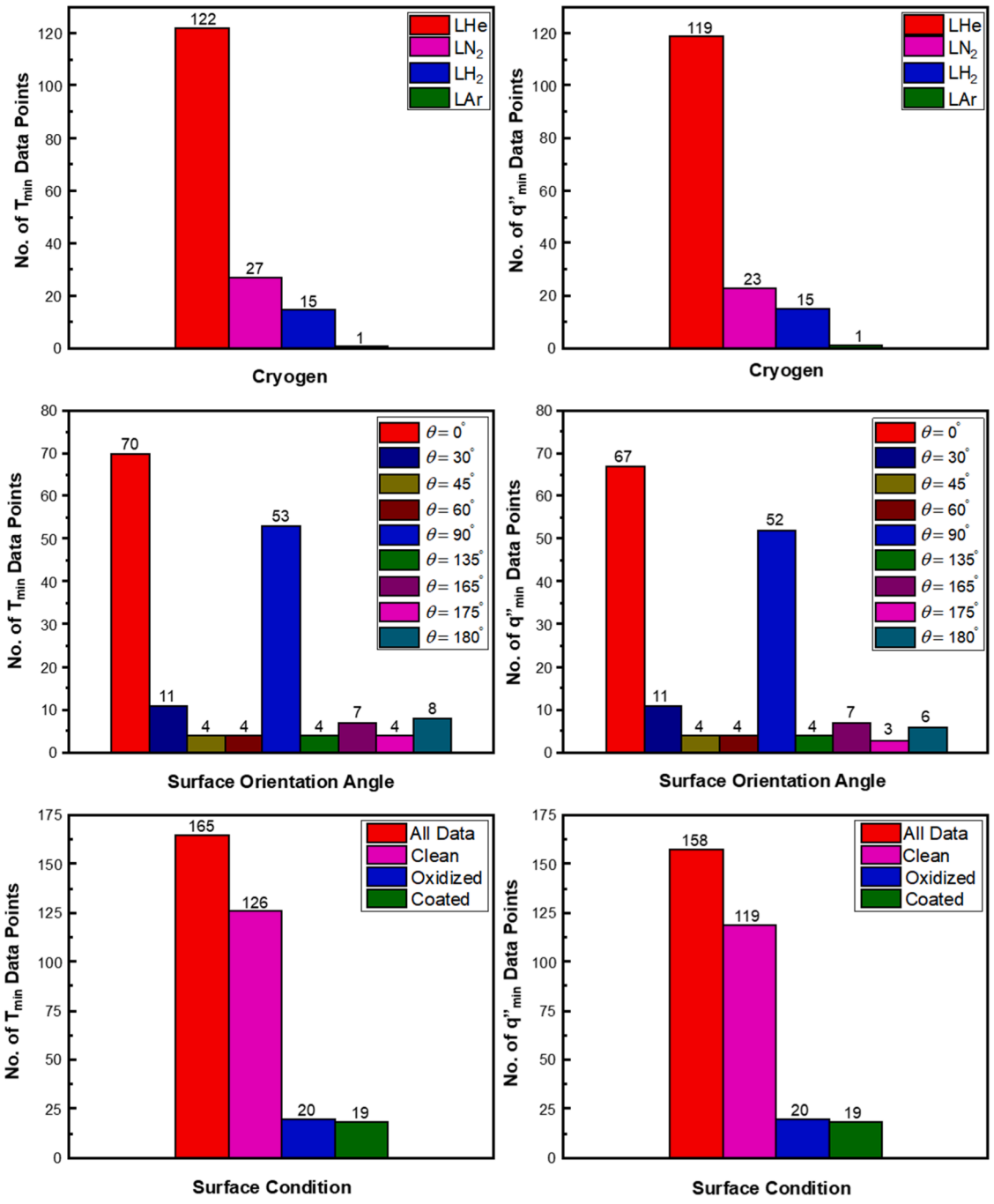

Fig. 5. Distribution of Consolidated Databases of T_{min} and q''_{min} based on cryogen, surface orientation, and surface condition.

MHF phenomenon. Upon thorough examination of published literature, it became apparent that researchers have predominantly pursued two distinct approaches in developing predictive tools for the MHF point. The first, known as the *thermodynamic* or *temperature-controlled* approach, has shown less frequent adoption compared to the second, *hydrodynamic* or *heat flux-controlled* approach.

The initial groundwork for the first approach was established by Spiegler et al. [27] in 1963. They introduced a straightforward yet impactful correlation for predicting T_{min} which involved a thermodynamic analysis based on the Van der Waals equation. They postulated that solid-liquid contact will occur when the temperature at the interface falls below the "foam" limit, which represents the maximum temperature the liquid can reach before film boiling initiates. Spiegler's correlation, T_{min}= 27 T_c / 32, which relies solely on the critical temperature (T_c) of the boiling fluid, stands as one of the simplest MHF correlations to date. While this approach faced criticism for lacking the effect of system pressure, it nonetheless marked a significant starting point for a new methodology that was subsequently refined by numerous researchers, as illustrated in Table 1. A similar strategy was adopted by Lienhard [32], who merged the Maxwell's criteria with the Van der Waals equation. Unlike Spiegler et al. [27], however, Lienhard incorporated the pressure effect via the fluid saturation temperature (T_{sat}). But despite considering effects of both the fluid critical temperature and system pressure, Lienhard's [32] correlation still fell short in addressing solid-liquid contact effects. Kalinin et al. [31] pursued an approach like Lienhard's while also accounting for thermal properties of the liquid and the heating surface: density, specific heat, and thermal conductivity, inclusion of which enabled predictions against available experimental

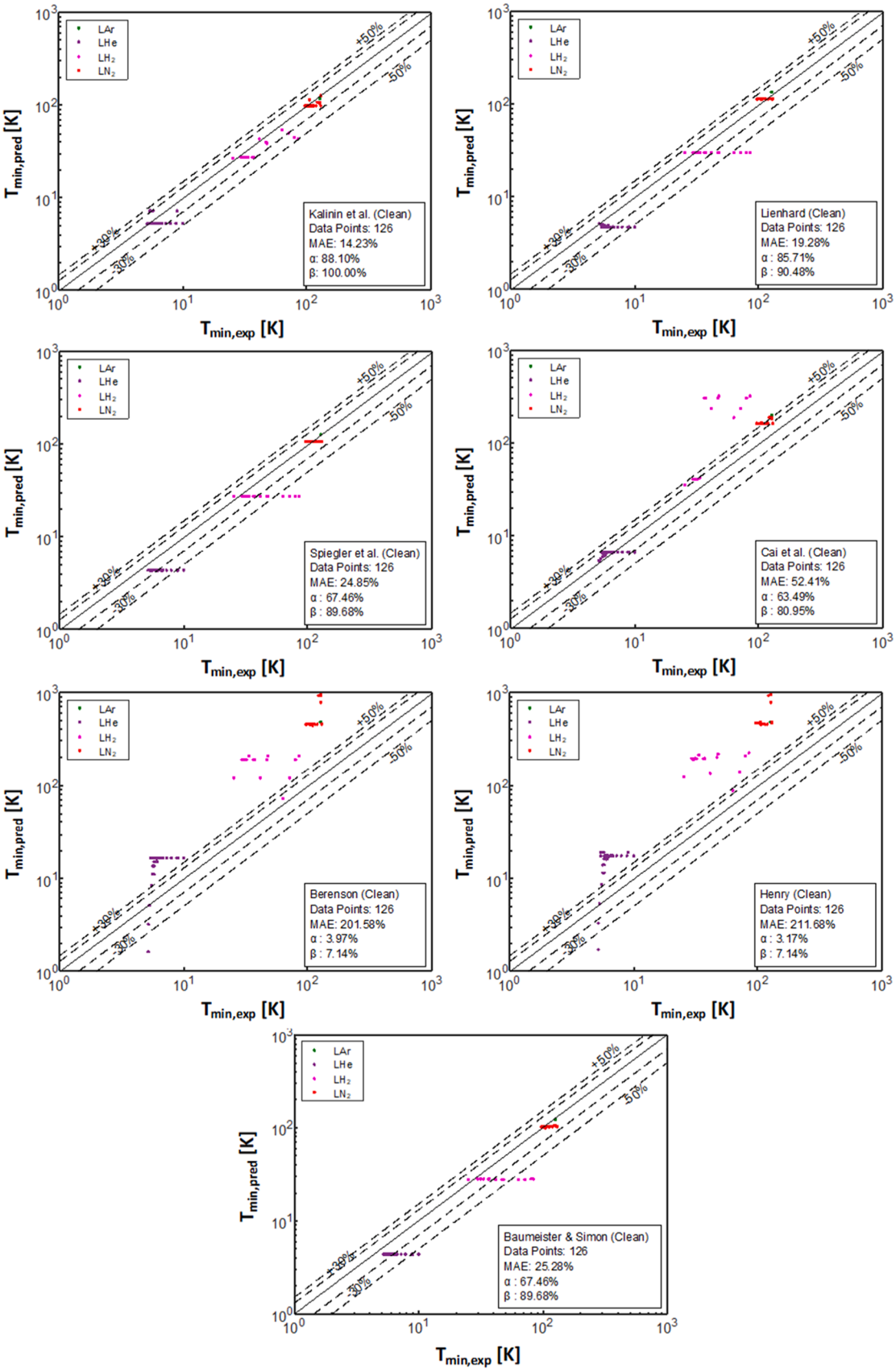

Fig. 6. Assessment of predictive accuracy of prior T_{min} correlations for clean surfaces.

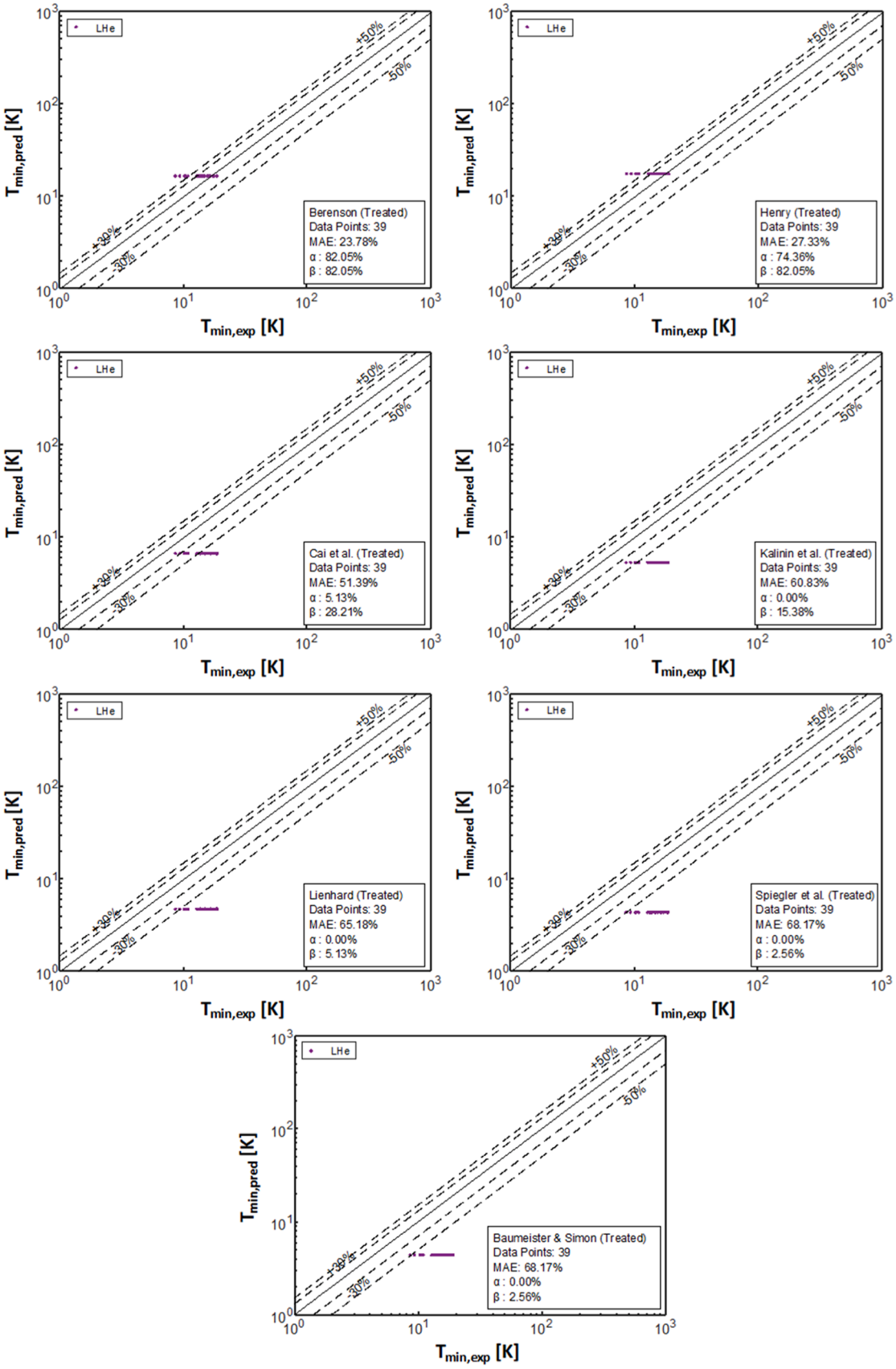

Fig. 7. Assessment of predictive accuracy of prior T_{min} correlations for treated (coated and oxidized) surfaces.

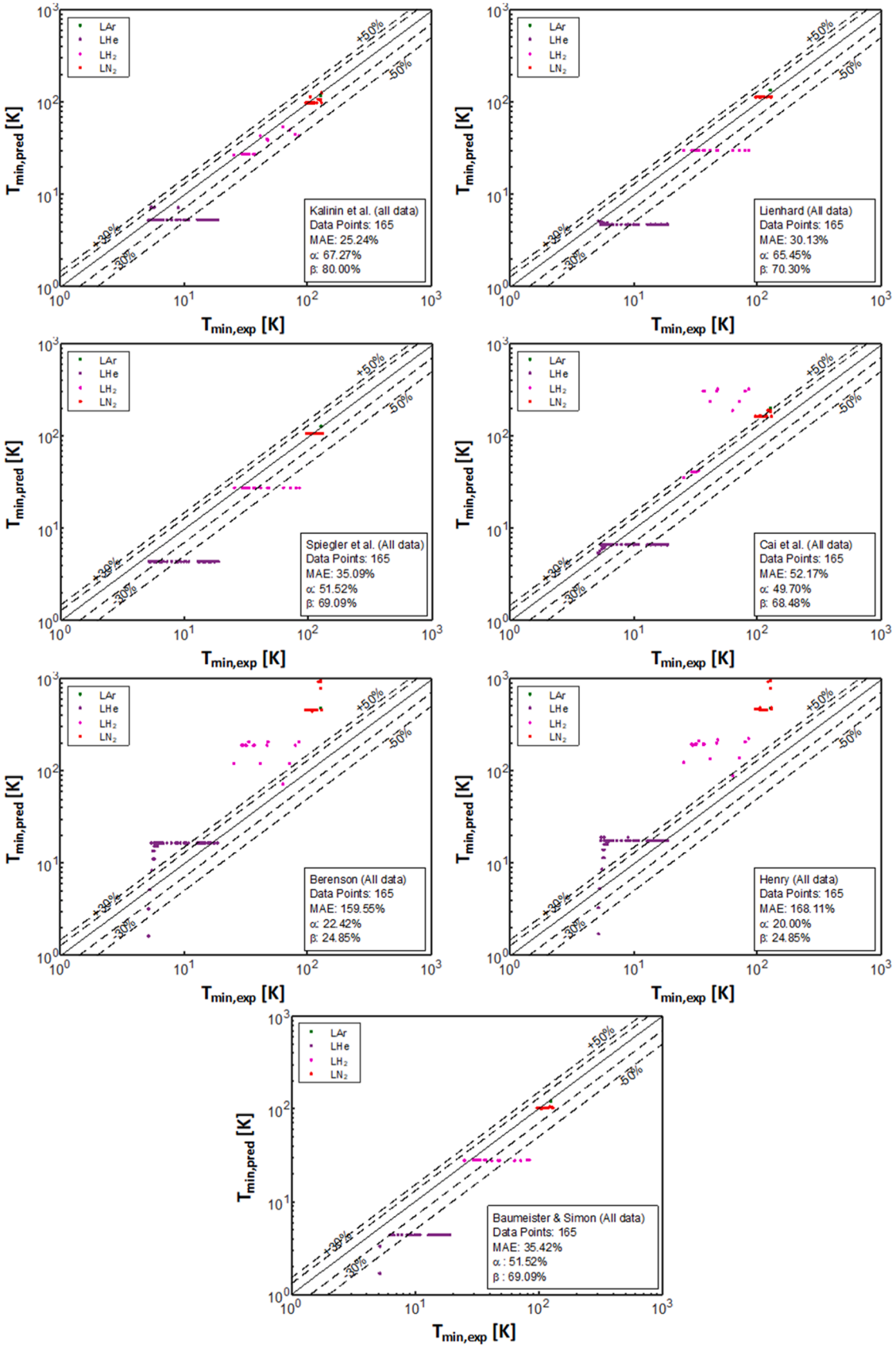

Fig. 8. Assessment of predictive accuracy of prior T_{min} correlations for all surfaces.

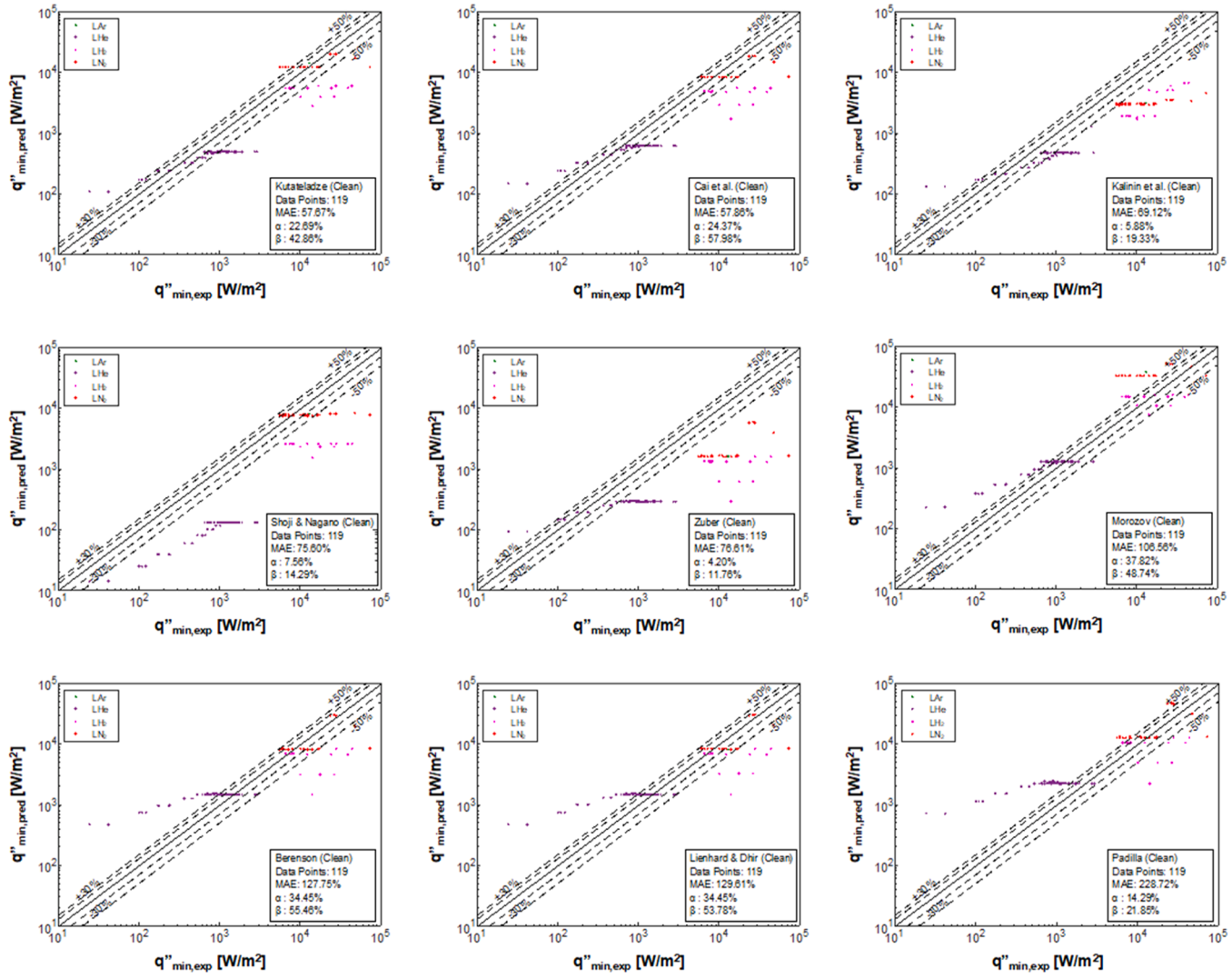

Fig. 9. Comparison of predictions of $q"_{min}$ correlations for clean surfaces.

data with an error margin of approximately ±20 %.

The other prevalent method for predicting MHF is the *hydrodynamic instability* approach, also known as the *heat flux-controlled* approach. This methodology, widely embraced within the research community, centers on the equilibrium of various forces, taking into consideration both interfacial instability and bubble dynamics. The cornerstone of this approach was laid by Kutateladze [35] in 1952. He utilized the equations of motion for the vapor film for both film boiling and transition boiling and postulated that film boiling would cease due to destruction of the continuous vapor layer, which he attributed to limited availability of vapor supply. He proposed that, at the MHF point, inertial forces acting on the vapor film surpass frictional forces, leading to the destruction of the vapor film. This assumption implies that the velocity of liquid in contact with the vapor is much smaller than the average velocity of the vapor layer. Subsequent to Kutateladze's work, Zuber [36] introduced another method to derive a correlation for $q"_{min}$. He suggested that vapor release from the heating surface can be approximated by spheres with a radius R equal to one-fourth the Taylor wavelength, which remains constant under constant pressure. He concluded that $q"_{min}$ is solely a function of bubble release frequency.

Building upon the pioneering work of Zuber [36], numerous researchers endeavored to develop correlations for $q"_{min}$ using similar functional forms but with adjustments to constants aimed at enhancing predictive accuracy. Details of these correlations are provided in Table 2. A notable approach was undertaken by Berenson [28], who adopted the Taylor instability in modeling the vapor film thickness. Berenson postulated that heat is transferred across a thin vapor layer via conduction. Initially, he devised a correlation for the HTC in the film boiling region and subsequently utilized Newton's law of cooling to formulate correlations for the MHF point, both T_{min} and $q"_{min}$. Henry [30] later noted that Berenson's correlation underestimates T_{min}. To correct this shortcoming, he incorporated the effects of thermal properties of both the fluid and heated surface into Berenson's model, thereby achieving improved predictive accuracy.

In a recent study, Cai et al. [12] employed a mechanistic approach to model MHF, conducting a force balance analysis on a unit cell of the wavy liquid-vapor interface over a flat horizontal surface. They postulated that the interface is dominated by the Taylor instability. As depicted in Fig. 3, Cai et al. postulated that the distance between two wave peaks equals the critical Taylor wavelength and any wave exceeding this wavelength would lead to vapor rupture. Their force balance analysis accounted for the effects of stagnation pressure on the underside of the wave and surface tension; both tend to stabilize the interface. Acting in a direction perpendicular to, and toward the surface are buoyancy force and pressure force resulting from the interfacial curvature; both tend to destabilize the interface. The net effect of stabilizing and destabilizing forces was shown to determine whether the system remains in the film boiling region or switches to the transition

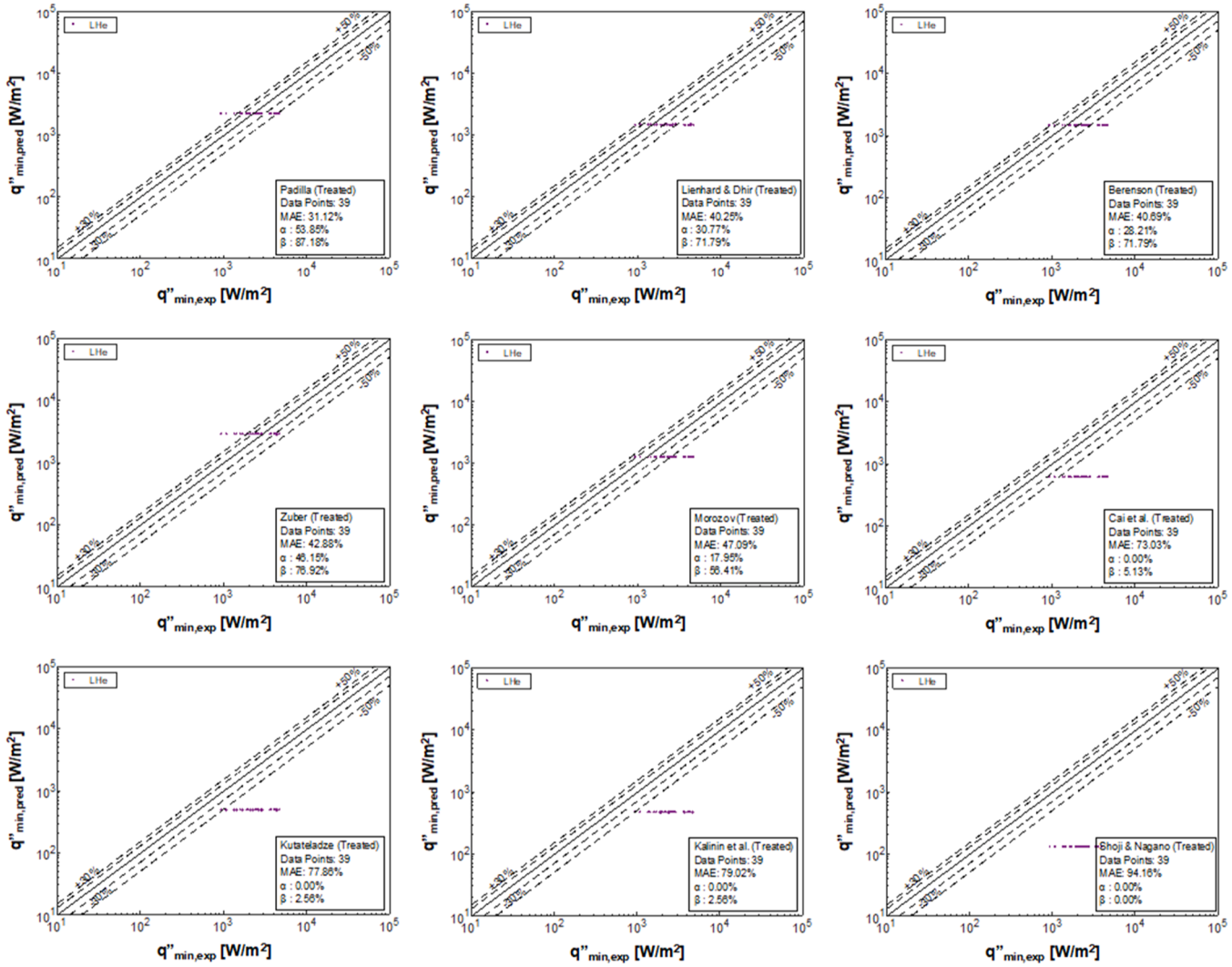

Fig. 10. Comparison of predictions of q"$_{min}$ correlations for treated (coated and oxidized) surfaces.

boiling region. The MHF point was postulated to occur when the four forces are in balance. Based on these postulates, Cai et al. developed a correlation for $q"_{min}$ and then utilized a HTC relation by Klimenko [42] to derive a correlation for T_{min}.

Fig. 4 provides the number of T_{min} and $q"_{min}$ correlations published per decade since 1950. As discussed above, most prior researchers focused on developing correlations for either T_{min} or $q"_{min}$ but some opted to use their $q"_{min}$ correlation to derive a correlation for T_{min} through application of Newton's law of cooling. However, Kalinin et al. [31] took a distinct approach by developing a correlation for T_{min} that incorporates effects of the thermal properties of both heating surface and fluid. They then employed the T_{min} correlation, alongside vapor properties, to derive a correlation for $q"_{min}$. This approach can be justified by the fact (as will be shown later) that available experimental T_{min} data show far less scatter than $q"_{min}$ data. This is why the present authors have opted to use a similar methodology to develop their new correlations for MHF.

3. New consolidated database for MHF point for saturated pool boiling of cryogens

3.1. Compilation of MHF point data and criteria for data exclusions

The present study employs a systematic approach to collect globally available MHF data for cryogenic fluids, including LHe, LN_2, LH_2, and LAr. This study uses a methodology for amassing published pool boiling MHF data like one employed by Ganesan et al. [2] for flow boiling. Key sources for the MHF data include scholarly articles from publishers like Elsevier and Springer, conference papers, NASA Technical Notes, and theses sourced globally. The MHF data are either extracted from graphical representations in the published literature using WebPlotDigitizer [43] or directly from tables. Some sources that were not available online were accessed through Purdue University's Interlibrary Loan (ILL) services.

Given this study's focus on saturated pool boiling from flat surfaces, deliberate exclusion criteria were applied, omitting data pertaining to pool boiling on spheres, tubes, cylinders, wires, or narrow channels. Following the initial elimination of duplicate data, further screening was carried out to exclude additional data that do not meet specific criteria:

1. Fluid Composition: Only data for pure cryogenic fluids are considered. Data for fluid mixtures or non-cryogenic fluids are excluded from consideration.
2. Boiling Region: Only MHF data are considered. A careful effort was exercised to avoid including any film boiling or transition boiling data.
3. Surface Heating: Any data other than for uniformly heated flat surfaces are excluded.

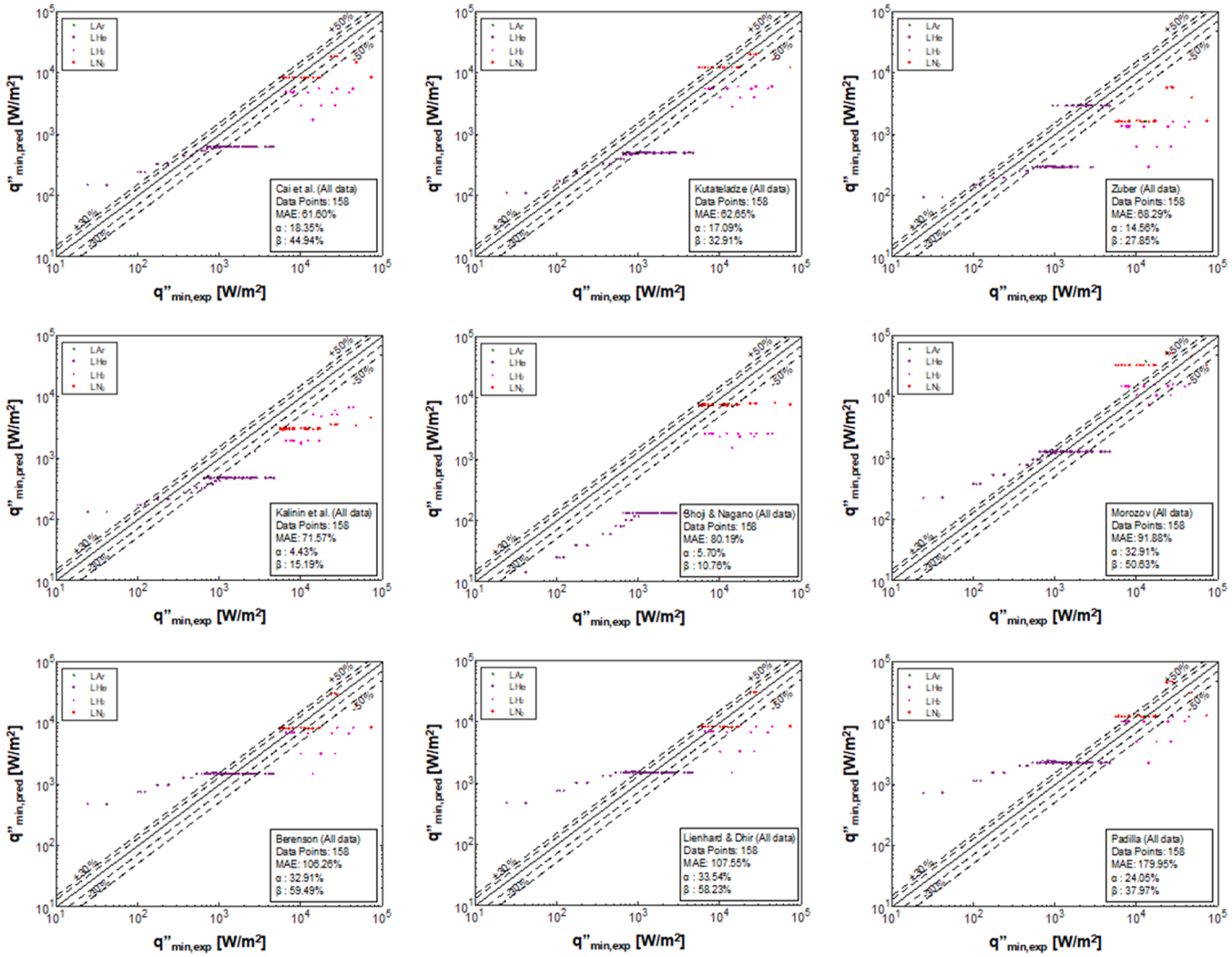

Fig. 11. Comparison of performances of $q"_{min}$ correlations for all data (clean, coated, and oxidized).

4. Boiling State: Since the present study is focused only on steady-state saturated boiling, quenching and subcooled data are excluded from consideration.
5. Pressure Conditions: The current study is focused entirely on subcritical pressures; data for supercritical conditions or subcooled liquids are excluded from consideration.
6. Surface Orientation: While the present study is focused mostly on horizontal and vertical surface orientations, given the sparsity of MHF data, other orientations are also considered.
7. Gravity Conditions: Only MHF data acquired in Earth gravity are considered; data for high-gravity and microgravity will be considered in a future study.
8. Surface Characteristics: Data from smooth, coated, oxidized, and micro-roughened surfaces are considered, while finned surface data are excluded.
9.Completeness of information: Only data available with complete information on operating conditions, such as operating pressure, heat flux, wall superheat, and orientation angle are considered. Data missing such complete information are excluded.

Application of these criteria yielded a meticulously curated database, Table 3, that is conducive to comprehensive analysis and correlation development.

3.2. Final consolidated database for MHF point for cryogens

While aiming to acquire the maximum number of datapoints for MHF condition, the present authors realized that, unlike nucleate boiling, film boiling, and CHF, for which extensive databases are available, MHF data for cryogens are unusually sparse. As discussed in the previous section and detailed in Table 3, 209 data points were amassed from 22 sources, but 44 points were excluded based on the above-mentioned criteria. The retained datapoints constitute the Consolidated Database which will be used hereafter to explore parametric trends, assess the accuracy of prior correlations, and formulate new correlations for both T_{min} and $q"_{min}$. Detailed in Table 4, the Consolidated Database comprises a total of 165 data points for T_{min} and 158 for $q"_{min}$, with the following distribution: LHe (122), LN_2 (27), LH_2 (15), and LAr (1). Moreover, the distribution of the data relative to surface orientation is as follows: $\theta = 0°$ (70), 30° (11), 45° (4), 60° (4), 90° (53), 135° (4), 165° (7), 175° (4), and 180° (8), where $\theta = 0°$ designates the horizontal upward-facing surface orientation. The database is also segregated based on surface condition: of 165 datapoints, 126 are for clean surfaces, 20 oxidized, and 19 coated. A detailed summary of the Consolidated Database is presented in Fig. 5 based on cryogen, orientation, and surface condition. It should be noted that the data excluded from the present study (subcooled, quenching, and non-Earth gravity) will be the focus of the authors' future work.

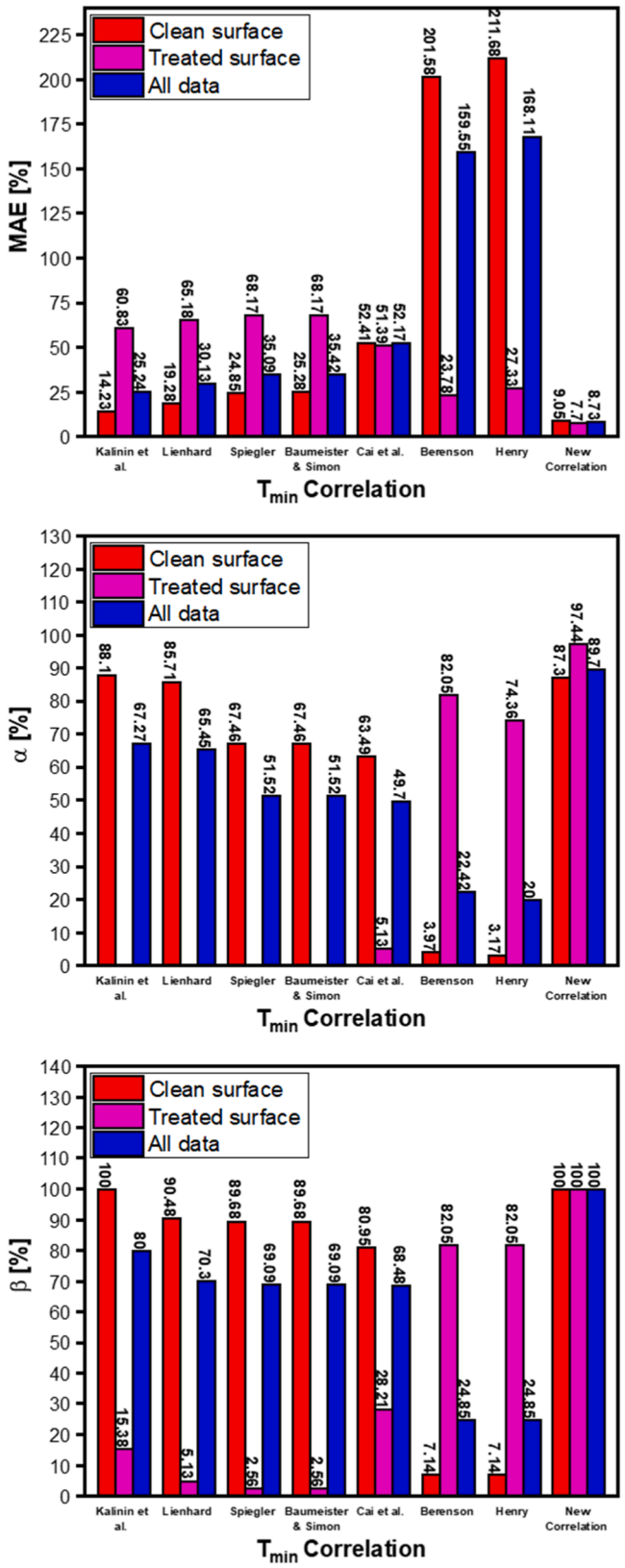

Fig. 12. Summary of statistical parameters for T_{min} correlations.

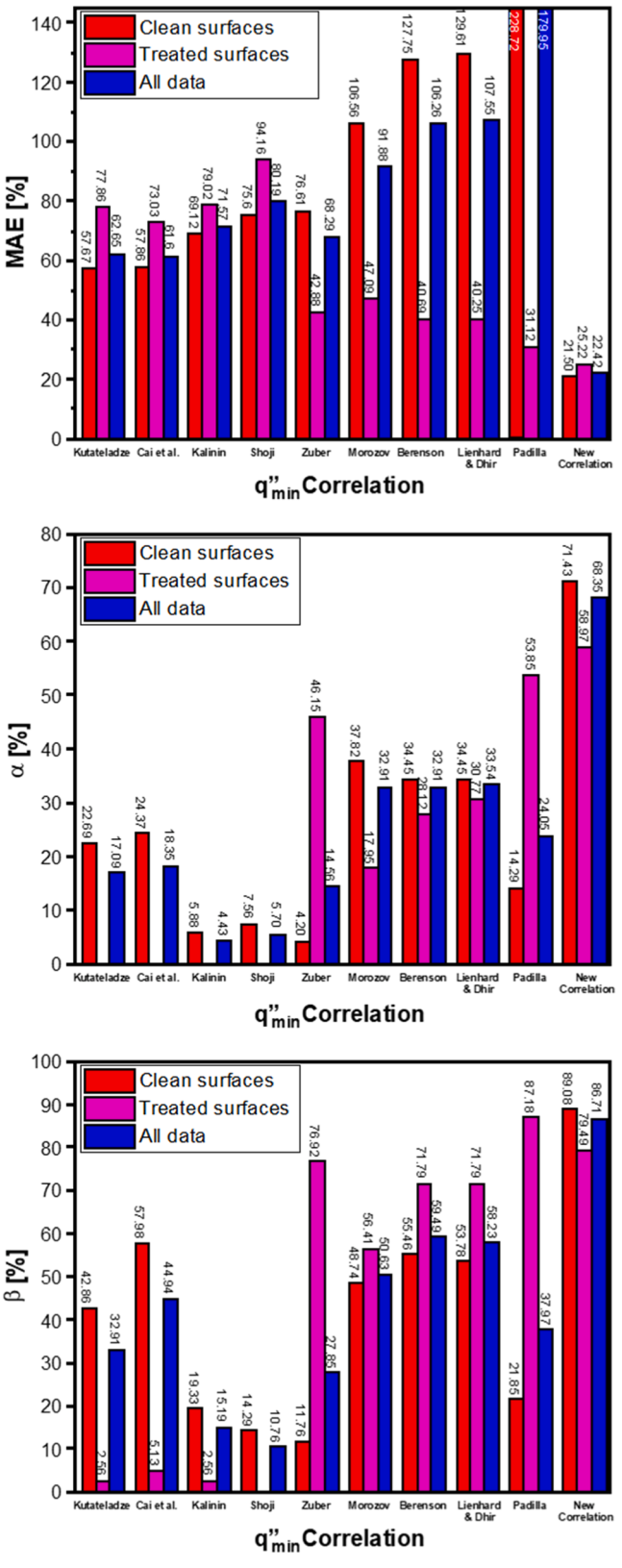

Fig. 13. Summary of statistical parameters for $q"_{min}$ correlations.

Table 5
Performance summary of best prior T_{min} correlations compared to the new correlation.

	Author(s)	MAE [%]	Predictions within ±30 (α) [%]	Predictions within ±50 (β) [%]	No. of data points
Clean surfaces					
1	Kalinin et al. [31]	14.23	88.10	100	126
2	Lienhard [32]	19.28	85.71	90.48	126
3	Spiegler et al. [27]	24.85	67.46	89.68	126
4	Baumeister and Simon [29]	25.28	67.46	89.68	126
5	Cai et al. [12]	52.41	63.49	80.95	126
6	Berenson [28]	201.58	3.97	7.14	126
7	Henry [30]	211.68	3.17	7.14	126
New Correlation					
		9.05	**87.30**	**100**	**126**
Treated surfaces					
1	Kalinin et al. [31]	60.83	0	15.38	39
2	Lienhard [32]	65.18	0	5.13	39
3	Spiegler et al. [27]	68.17	0	2.56	39
4	Baumeister and Simon [29]	68.17	0	2.56	39
5	Cai et al. [12]	51.39	5.13	28.21	39
6	Berenson [28]	23.78	82.05	82.05	39
7	Henry [30]	27.33	74.36	82.05	39
New Correlation					
		7.70	**97.44**	**100**	**39**
All data, including clean and treated surfaces					
1	Kalinin et al. [31]	25.24	67.27	80	165
2	Lienhard [32]	30.13	65.45	70.30	165
3	Spiegler et al. [27]	35.09	51.52	69.09	165
4	Baumeister and Simon [29]	35.42	51.52	69.09	165
5	Cai et al. [12]	52.17	49.70	68.48	165
6	Berenson [28]	159.55	22.42	24.85	165
7	Henry [30]	168.11	20	24.85	165
New Correlation					
		8.73	**89.70**	**100**	**165**

Table 6
Performance summary of prior q"$_{min}$ correlations compared to the new correlation.

	Author(s)	MAE [%]	Predictions within ±30 (α), [%]	Predictions within ±50 (β), [%]	No. of data points
Clean surfaces					
1	Kutateladze [35]	57.67	22.69	42.86	119
2	Cai et al. [12]	57.86	24.37	57.98	119
3	Kalinin et al. [31]	69.12	5.88	19.33	119
4	Shoji and Nagano [41]	75.60	7.56	14.29	119
5	Zuber [36]	76.61	4.20	11.76	119
6	Morozov [37]	106.56	37.82	48.74	119
7	Berenson [28]	127.75	34.45	55.46	119
8	Lienhard and Dhir [40]	129.61	34.45	53.78	119
9	Padilla [38]	228.72	14.29	21.85	119
New Correlation					
		21.50	**71.43**	**89.08**	**119**
Treated surfaces					
1	Kutateladze [35]	77.86	0	2.56	39
2	Cai et al. [12]	73.03	0	5.13	39
3	Kalinin et al. [31]	79.02	0	2.56	39
4	Shoji and Nagano [41]	94.16	0	0	39
5	Zuber [36]	42.88	46.15	76.92	39
6	Morozov [37]	47.09	17.95	56.41	39
7	Berenson [28]	40.69	28.12	71.79	39
8	Lienhard and Dhir [40]	40.25	30.77	71.79	39
9	Padilla [38]	31.12	53.85	87.18	39
New Correlation					
		25.22	**58.97**	**79.49**	**39**
All data, including clean and treated surfaces					
1	Kutateladze [35]	62.65	17.09	32.91	158
2	Cai et al. [12]	61.60	18.35	44.94	158
3	Kalinin et al. [31]	71.57	4.43	15.19	158
4	Shoji and Nagano [41]	80.19	5.70	10.76	158
5	Zuber [36]	68.29	14.56	27.85	158
6	Morozov [37]	91.88	32.91	50.63	158
7	Berenson [28]	106.26	32.91	59.49	158
8	Lienhard and Dhir [40]	107.55	33.54	58.23	158
9	Padilla [38]	179.95	24.05	37.97	158
New Correlation					
		22.42	**68.35**	**86.71**	**158**

4. Assessment of prior models and correlations

4.1. Statistical parameters and assessment methodology

The Consolidated Database stands as a crucial tool for assessing the predictive capability of all the above-mentioned correlations in projecting the MHF point. This exhaustive evaluation entails the utilization of mean absolute error (MAE) which is calculated as:

$$MAE = \frac{1}{N}\sum \frac{|Predicted\ value - Experimental\ value|}{Experimental\ value} \times 100\% \quad (1)$$

where N is the total number of data points for which the correlations are evaluated, experimental value is taken from the Consolidated Database, and predicted value is calculated using the tested correlation. Since MAE is an average measure and may not capture the complete picture of how a correlation performs, two additional statistical parameters are also employed: percentage of predictions of a correlation within ±30 % (α) of the data, and percentage predicted within ±50 % (β).

4.2. Assessment and comparison of prior correlations

Before embarking on the development of a novel correlation for MHF, it is imperative to assess the accuracy of the previously published correlations and grasp the significance of certain parameters. In the subsequent sections, correlations for T_{min} and $q"_{min}$ will be evaluated and compared separately.

4.2.1. Comparison of T_{min} correlations

As mentioned earlier, it is necessary to segregate the Consolidated Database relative to surface condition, given strong impact of this parameter on MHF. To do so, the data for clean and unclean (coated and oxidized) surfaces are examined separately. Fig. 6 compares predictions of seven different T_{min} correlations, which include both thermodynamic and hydrodynamic formulations, against 126 clean surface data points of the Consolidated Database. It can be seen that the correlation by Kalinin et al. [31], having a MAE of 14.33 %, outperforms all others. It is followed in order of best T_{min} predictions by Lienhard [32], Spiegler et al. [27], Baumeister and Simon [29], and Cai et al. [12], having MAEs of 19.28 %, 24.85 %, 25.28 %, and 52.41 %, respectively. On the other hand, with MAEs exceeding 200 %, the correlations by Berenson [28] and Henry [30] lag significantly behind in ability to accurately predict

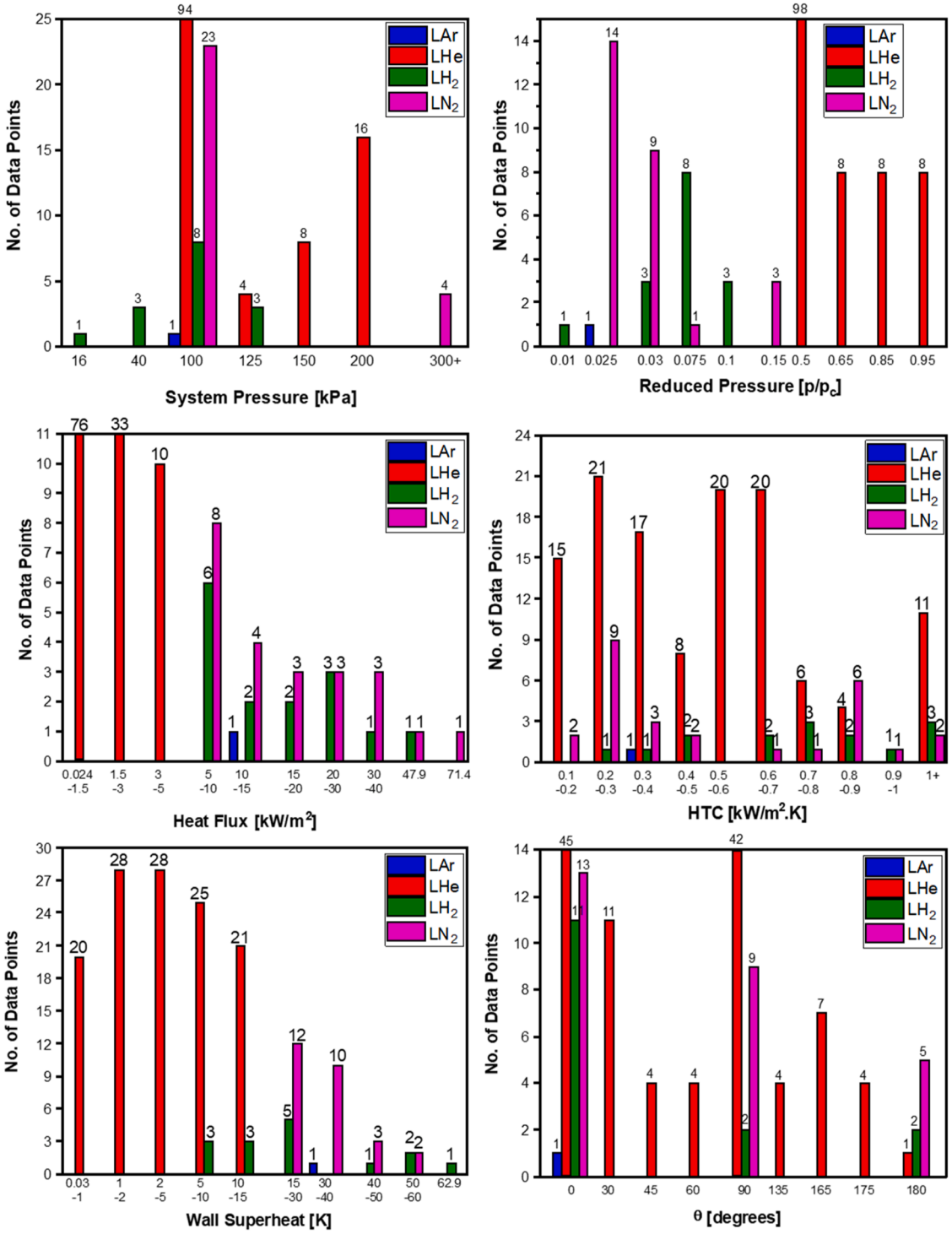

Fig. 14. Parametric distribution of Consolidated Database.

the data.

A deeper investigation revealed differences in the performance of correlations for different surface materials (copper, stainless steel, and aluminum). What sets Kalinin et al.'s [31] apart from others in terms of predictive performance is incorporation of thermal properties of both the heating surface and fluid.

With 39 treated surface data points (20 for oxidized and 19 for coated) from the Consolidated Database, the same six correlations are re-evaluated, this time for treated surfaces. Fig. 7 reveals a virtual reversal in the order of best performing correlations. With respective MAEs of 23.78 % and 27.33 %, Berenson's [28] and Henry's [30] yielded the best performance, while those of Cai et al. [12], Kalinin et al. [31], Lienhard [32], Baumeister and Simon [29], and Spiegler et al. [27], with MAEs of 51.39 %, 60.83 %, 65.18 %, 68.17 %, and 68.17 %, respectively, showed more appreciable departure from the data.

To conduct an overall assessment of T_{min} correlations, the data for both the clean and treated surfaces are aggregated, denoted as "all data," and the results are depicted in Fig. 8. It is evident that trends in Fig. 8 resemble those in Fig. 6 more than in Fig. 7. This is attributed to the clean surface T_{min} data points comprising majority of the Consolidated

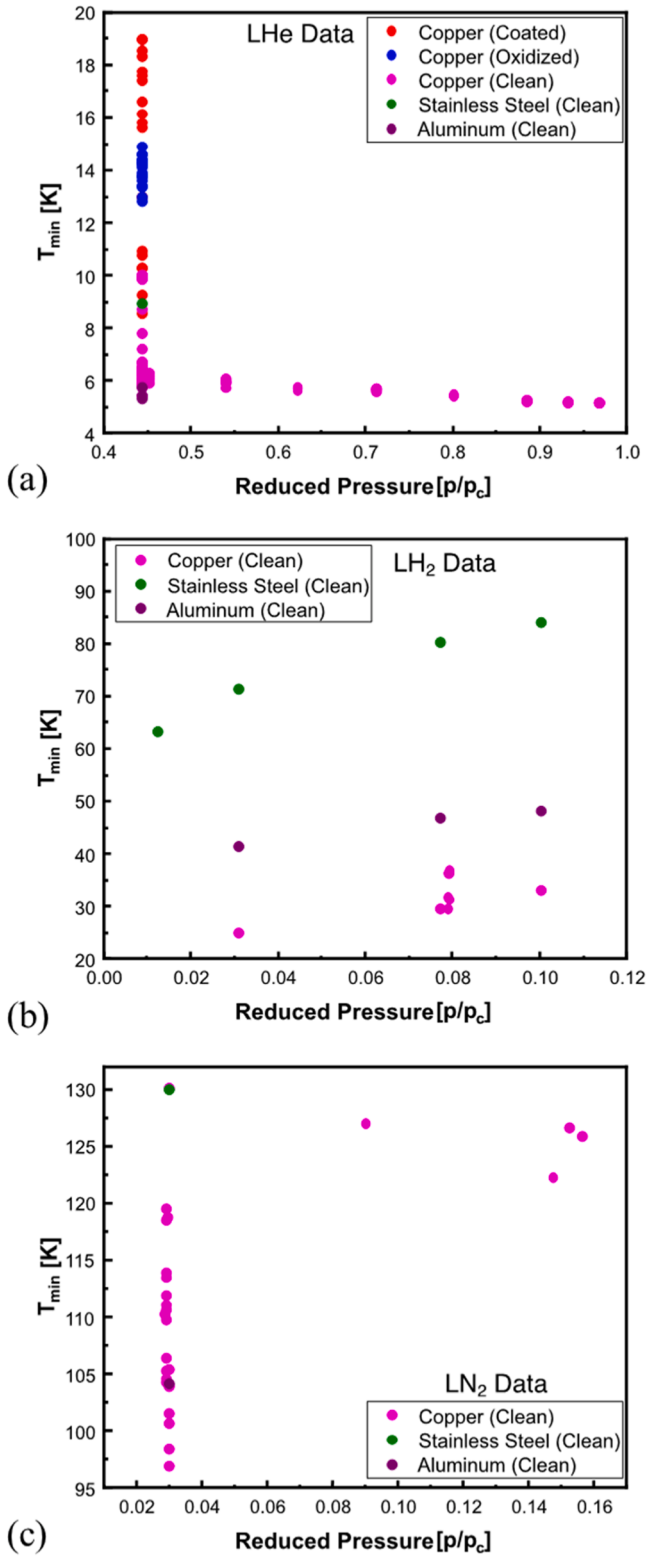

Fig. 15. Deviations in T_{min} data for (a) LHe, (b) LH_2, and (c) LN_2.

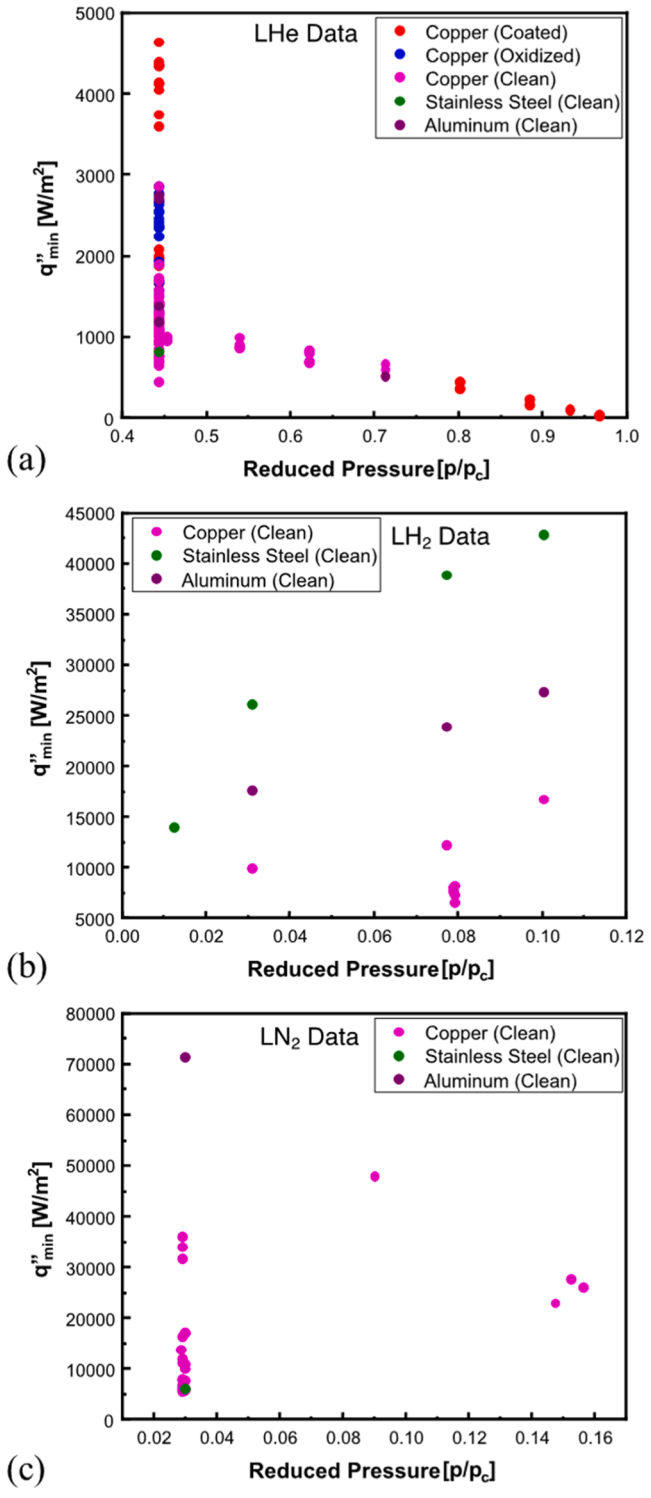

Fig. 16. Deviations in q"$_{min}$ data for (a) LHe, (b) LH_2, and (c) LN_2.

Database. Fig. 8 shows the Kalinin et al.'s [31] correlation, with a MAE of 25.24 %, yields best overall performance. It is followed in order by Lienhard [32] (30.13 %), Baumeister and Simon [29] (35.42 %), Spiegler et al. [27] (35.09 %), Cai et al. [12] (52.17 %), Berenson [28] (159.55 %), and Henry [30] (168.11 %).

The seemingly contradictory trends between Figs. 6 and 7 underscore the significance of considering surface condition when developing a new correlation for T_{min}.

4.2.2. *Comparison of q"$_{min}$ correlations*

In this section, a methodology like that employed for evaluating T_{min} correlations in the preceding section is adopted. Here, focus shifts to comparing the outcomes of nine distinct correlations for $q"_{min}$. The Consolidated Database utilized for this analysis comprises a total of 158 data points, with 119 data points for cleaned surfaces and 39 for treated (oxidized and coated).

Table 7
New correlations for T_{min} and $q"_{min}$.

$$T_{\min} = \left[T_{sat} + (T_c - T_{sat})\left(-9.1 + 12\left(\frac{k_f\rho_f c_{p,f}}{k_w\rho_w c_{p,w}}\right)^{0.025}\right)\right] S_T$$

where S_T is the surface characteristics multiplier:
For clean surfaces: $S_T = 1$
For oxidized surfaces: $S_T = 2.3$
For coated surfaces: $S_T = \frac{(\delta - 1.2999\times10^{-6})^{0.042}}{(0.06k_c)^{0.247}(\theta+0.2)^{0.012}}$

$$q"_{min} = 0.043\left[\frac{c_{p,g}k_g^2}{\mu_g}\rho_g g(\rho_f-\rho_g)\right]^{0.567}\left\{-0.107 + 0.38\,(\Delta T_{min})^{0.39}\right\}^{3.094} S_q$$

where

$$\Delta T_{min} = (T_c - T_{sat})\left(-9.1 + 12\left(\frac{k_f\rho_f c_{p,f}}{k_w\rho_w c_{p,w}}\right)^{0.025}\right)$$

and S_q is the surface characteristics multiplier:
For clean surfaces: $S_q = 1$
For oxidized surfaces: $S_q = 2.18$
For coated surfaces: $S_q = \frac{(\delta - 1.28\times10^{-6})^{0.1}}{(0.132k_c)^{0.43}(\theta+0.05)^{0.07}}$

Unlike the T_{min} correlations, MAEs of the $q"_{min}$ correlations are comparatively quite high, indicating difficulty of predicting $q"_{min}$ compared to T_{min}. This is due to the wide distribution of values for $q"_{min}$ from experiments, which will be discussed in more detail in Section 5.

Fig. 9 shows a comparison of $q"_{min}$ correlations for clean surface data. The correlations can be loosely segregated into two groups: one featuring MAEs below 80 % and another above 100 %. The correlations of Kutateladze [35] and Cai et al. [12], with MAEs of 57.67 % and 57.86 %, respectively, outperform all prior correlations. They are followed among the first group in order of predictive accuracy by the correlations of Kalinin et al. [31], Shoji and Nagano [41], and Zuber [36], having MAEs of 69.12 %, 75.60 %, and 76.61 %, respectively. The second group consists of four correlations: Morozov [37], Berenson [28], Lienhard and Dhir [40], and Padilla [38], which feature comparatively high MAEs of 106.56 %, 127.75 %, 129.61 %, and 228.72 %, respectively.

Similar to the clean surface data, the $q"_{min}$ correlations are tested in Fig. 10 against the treated surface data, including both oxidized and coated surfaces, which are available only for LHe. Here too, the correlations can be categorized into two groups based on MAE. Unexpectedly, the performance of the first group of five correlations is much better for treated surfaces than for clean surfaces, evidenced by all five correlations having MAEs below 50 %. With a MAE of 31.12 %, the correlation of Padilla [38] shows best performance, followed in order by Lienhard and Dhir [40], Berenson [28], Zuber [36], and Morozov [37], having MAEs of 40.25 %, 40.69 %, 42.88 %, and 47.09 %, respectively. But, despite their comparatively low MAEs, these correlations show unusual predictions along an almost horizontal line. This implies the correlations provide a single predicted value corresponding a range of experimental values. As discussed earlier, this is reflective of the broader spread of $q"_{min}$ data compared to the T_{min} data as noted by authors of several experimental MHF studies. Also shown in Fig. 10 are performance assessments of the second group of correlations against the treated clean surface data. This group consists of four correlations: Cai et al. [12], Kutateladze [35], Kalinin et al. [31], and Shoji and Nagano [41], which feature comparatively high MAEs of 73.03 %, 77.86 %, 79.02 %, and 94.16 %, respectively.

To capture a comprehensive overview, the data from both clean and treated surfaces are combined and referred to as "all data," comprising a total of 158 data points for $q"_{min}$. A comparison of performances of the $q"_{min}$ correlations in provided in Fig. 11. The first group of four best performing correlations, having MAE values below 80 %, against all data encompass Cai et al. [12], Kutateladze [35], Zuber [36], and Kalinin et al. [31], which feature MAEs of 61.60 %, 62.65 %, 68.29 %, and 71.57 %, respectively. The comparatively elevated MAEs of these correlations can be attributed to the wide dispersion of $q"_{min}$ data and inclusion of both clean and treated surface data. The subsequent five correlations comprise Shoji and Nagano [41], Morozov [37], Berenson [28], Lienhard and Dhir [40], and Padilla [38], having MAEs of 80.19 %, 91.88 %, 106.26 %, 107.55 %, and 179.95 %, respectively.

In conclusion, the evaluation of T_{min} and $q"_{min}$ correlations for both clean and treated surfaces provides valuable insights into predictive capabilities in the context of saturated pool boiling of cryogenic fluids. While certain correlations demonstrate promising performance under specific conditions, others exhibit serious limitations. The significant discrepancies observed highlight the complexity of predicting T_{min} and $q"_{min}$ and underscore the need for further refinement and development of new, improved correlations.

4.3. Summary of statistical results of prior predictive tools

In the preceding sections, we meticulously examined prediction outcomes for better performing prior correlations for both T_{min} and $q"_{min}$. To summarize findings from this analysis, the prior correlations (along those of the new correlations to be discussed in subsequent sections), are compared in terms of MAE and predictions falling within ±30 % (α) and ±50 % (β) of the data, first for T_{min} in Fig. 12 and subsequently for $q"_{min}$ in Fig. 13, with more quantitative information provided in Tables 5 and 6, respectively.

Figs. 12 and 13 depict comparisons of performances of the T_{min} and $q"_{min}$ correlations, respectively, segregated each based on surface condition. It is worth noting that superior performance is exemplified by lower value for MAE and higher values for both α and β. Upon careful examination of Figs. 12 and 13 and Tables 5 and 6, it apparent that the new correlations for both T_{min} and $q"_{min}$ to be discussed in subsequent sections provide both the lowest MAE values and the highest α and β values, underscoring their superior performances.

5. New universal correlations for MHF point for saturated pool boiling of cryogens

5.1. Parametric distribution of consolidated database

Before embarking on the development of new correlations for T_{min} and $q"_{min}$, it is crucial to thoroughly comprehend every facet of the Consolidated Database. To achieve this, the Consolidated Database is meticulously examined based on key parameters, namely system pressure, reduced pressure, heat flux, heat transfer coefficient (HTC), wall superheat, and surface orientation angle. Results are shown in Fig. 14.

It is apparent from Fig. 14 that majority of the data cluster around 100 kPa, which corresponds to near atmospheric pressure. However, because of low critical pressure, the LHe data are associated mostly with higher values of reduced pressure. Additionally, the LHe data tend to have lower heat flux values, while the LH_2 and LN_2 data higher values, which is reflection of distinct thermophysical properties of different cryogens. Furthermore, far more data are available for the horizontal upward facing and vertical surface orientations compared to the other orientations. Overall, the parametric distributions in Fig. 14 serve both as a valuable guide for understanding available data trends and provide a rational basis for recommending future cryogenic fluid experiments.

5.2. Recommendations for future work

After the thorough literature review in Section 1, the insights gained from the Consolidated Database in Section 3, and the parametric distributions presented in Fig. 14, several important recommendations emerge for future researchers interested in contributing new experimental work related to pool boiling MHF for cryogenic fluids:

i. Compared to nucleate boiling, CHF, and film boiling, the MHF point has gained very limited attention in published literature. Therefore, more focus needs to be devoted to this important

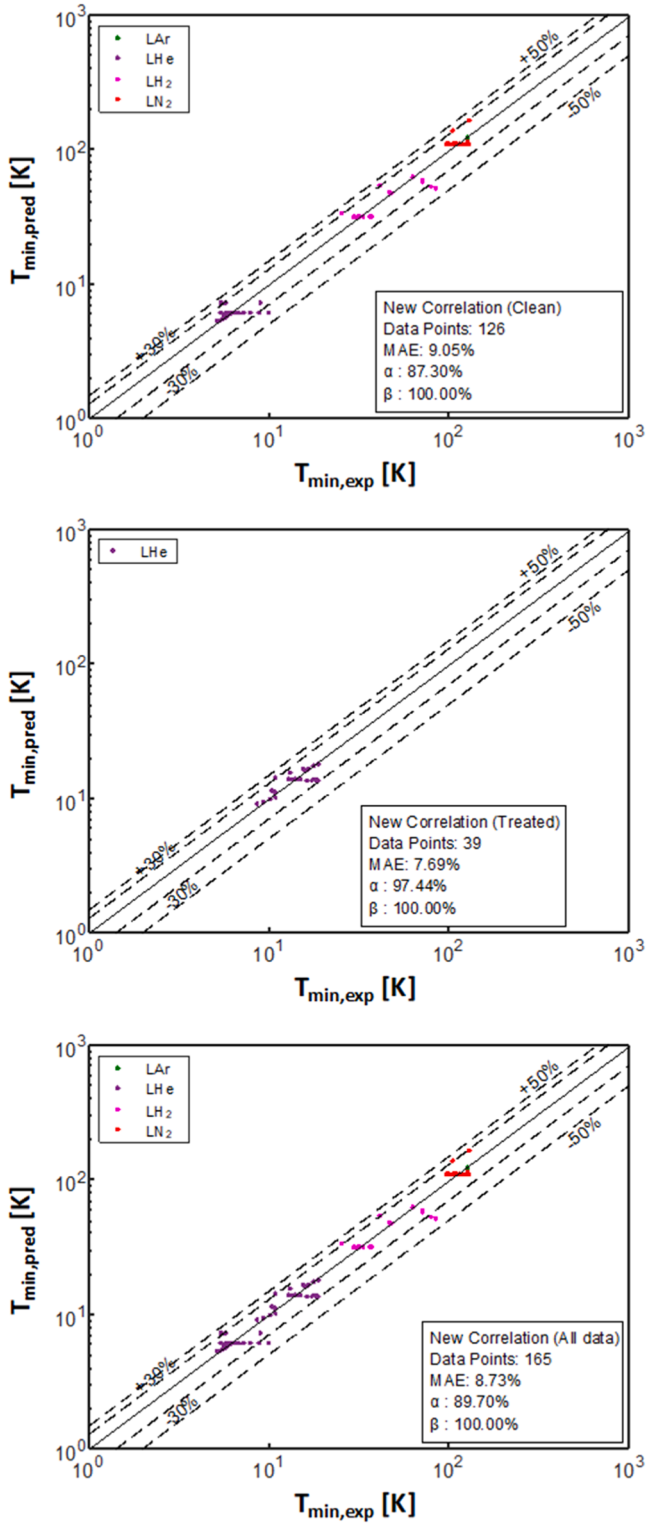

Fig. 17. Assessment of predictive accuracy of the new T_{min} correlation against data for clean surfaces, treated surfaces, and all surfaces combined.

phenomenon in pursuit of a more precise capture of the entire boiling curve.

ii. The MHF point is strongly dependent on surface characteristics which have received very limited attention in prior studies. Clearly, these effects are worthy of far more serious focus in the future to better understand their impact on both T_{min} and q''_{min}.

iii. The currently available MHF data are much more skewed towards LHe, with far fewer data points available for LH_2, LN_2, and especially LAr, and no data for LO_2 or LCH_4. Therefore, future researchers are advised to fill this data gap to ensure that future correlations will be universal to the entire family of cryogens.

iv. The consolidated database is also skewed towards horizontal upward facing and vertical surface orientations. Future experiments conducted in other orientations will contribute to formulating new correlations that will provide accurate predictions for the entire range of surface orientations.

v. Excepting LHe, no MHF data are available for the other cryogens above $0.16p_c$. Absence of such high-pressure data compromises the effectiveness of correlations at capturing MHF trends over the entire pressure range up to the critical point.

vi. The MHF point is strongly influenced by thermal properties of the heating wall. Yet, with limited relevant information from published works, the effectiveness of correlations in capturing this important influence is highly compromised and therefore far more serious attention is required in future work to address this influence.

5.3. Deviations in MHF point data

Before delving into the development of new correlations for T_{min} and q''_{min}, it is crucial to examine important deviations in both as reported in prior experimental works. While the parametric distributions of the Consolidated Database were presented in Fig. 14; however, Figs. 15 and 16 offer clearer insight into how the T_{min} and q''_{min} data vary with pressure. Due to significant disparities in T_{min} and q''_{min} values among different cryogens (for instance, the highest q''_{min} value for LHe is less than 5000 W/m^2, while values for LH_2 and LN_2 are above 5000 W/m^2), these variations are plotted separately for individual cryogens. Notably, LAr is intentionally excluded given only a single data point available for this cryogen as shown in Fig. 14.

Figs. 15 and 16 reveal substantial variations in values of both T_{min} and q''_{min} for each cryogen. As shown in Figs. 15(a) and 16(a), coated and oxidized surfaces are shown greatly increasing values of both MHF parameters for LHe compared to clean surfaces. And for LH_2, Figs. 15(b) and 16(b) also show large variations, which are attributed consistently to differences in surface material, with stainless steel (least conducting wall material) yielding highest T_{min} and q''_{min} values, followed in order by aluminum and copper (most conducting material). However, other deviations are more challenging to justify, as there is considerable spread in data for the same heating surface material and pressure, which has not been clearly elucidated by past researchers. For instance, as shown in Fig. 15(c), measured T_{min} values for LN_2 at atmospheric pressure ($0.03p_c$) ranges from 96 to 120 K, despite the surface material remaining same for all corresponding data points except two. Potential reasons for such deviations include discrepancies in heat flux incrementation or decrementation steps across different pool boiling experiments or within the same experiment. Heated surface size and thickness may be two additional causes, which, given the limited number of published data points, will require additional attention in future experimental endeavors.

Notably, the deviations in q''_{min} values across all cryogens are notably greater than those observed in T_{min} values. This discrepancy is responsible for prior q''_{min} correlations yielding significantly higher MAEs than T_{min} correlations, as discussed earlier. Therefore, it is imperative for readers to bear this in mind when investigating prior predictive tools or developing new correlations for MHF point. We also advocate that future researchers provide more comprehensive information about their experimental setup, instrumentation, operating procedure, and measurement accuracy, as this will enable other investigators to more accurately account for known and perhaps lesser-known influencing parameters.

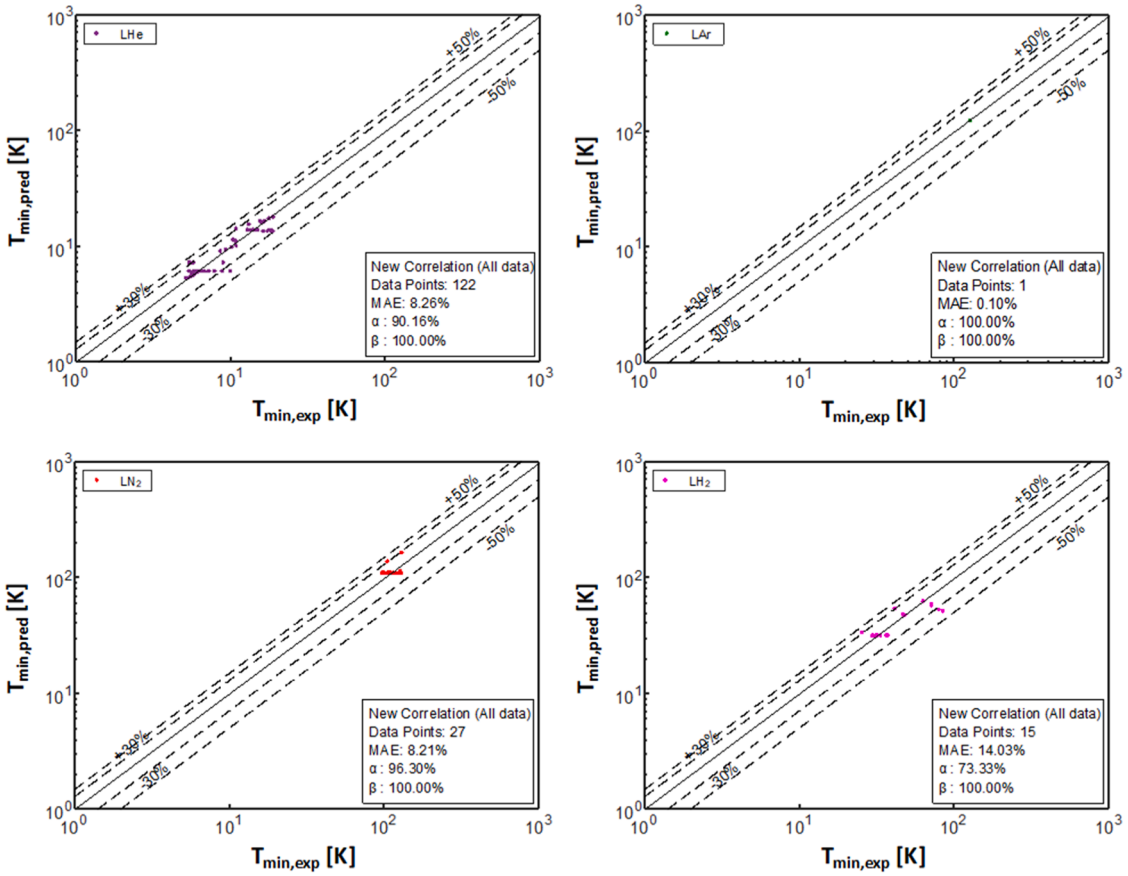

Fig. 18. Assessment of predictive accuracy of the new T_{min} correlation against data for individual cryogens.

5.4. New universal correlation for T_{min}

Development of new correlations entails a thorough investigation of prior experimental trends and previously published correlations. As discussed in Section 2, two techniques are commonly employed for developing correlations for T_{min}: the thermodynamic approach and the hydrodynamic approach. After conducting a meticulous assessment of prior works in Section 4.2, it became evident that the thermodynamic approach is more suitable for the T_{min} correlation. The groundwork for the thermodynamic approach was laid by Spiegler et al. [27], who introduced the following simple formulation:

$$T_{min} = \frac{27}{32} T_c \tag{2}$$

But, while this relation marked a significant starting point for the thermodynamic approach, it lacked consideration of operating conditions, such as pressure, which led to criticism from many authors. Subsequent researchers aimed to improve this correlation. For example, Lienhard [32] incorporated saturation temperature to address the pressure effects. Kalinin et al. [31] expanded upon Lienhard's work by incorporating both saturation temperature and thermal properties of both heating surface and fluid. Notably, the correlation proposed by Kalinin et al. [31] demonstrated promising performance, having a MAE of 14.23 % for clean surface data. Building upon this success, a regression analysis was conducted in the present study to refine the coefficients and exponents of Kalinin et al.'s correlation, aiming to further enhance its accuracy. Following is the new modified form for clean surfaces:

$$T_{min} = T_{sat} + (T_c - T_{sat}) \left(-9.1 + 12 \left(\frac{k_f \rho_f c_{p,f}}{k_w \rho_w c_{p,w}} \right)^{0.025} \right) \tag{3}$$

where T_c and T_{sat} are the fluid's critical and saturation temperatures (K), and k, ρ, and c_p represent thermal conductivity (W.m^{-1}.K^{-1}), density (kg.m^{-3}), and specific heat capacity (J.kg^{-1}.K^{-1}), respectively, with subscript f representing fluid and w heating surface. It should be noted that all properties of solid and fluid are evaluated at the saturation temperature of the liquid.

The above correlation was tested for both clean surfaces and treated surfaces (coated and oxidized), which proved that it is invalid for the latter because of the altered physics resulting from coating or oxidation. Hence, adjustments in the correlation are required to accommodate treated surfaces. To address this, a surface characteristics temperature multiplier S_T is introduced, resulting in the following new correlation for T_{min}.

$$T_{min} = \left[T_{sat} + (T_c - T_{sat}) \left(-9.1 + 12 \left(\frac{k_f \rho_f c_{p,f}}{k_w \rho_w c_{p,w}} \right)^{0.025} \right) \right] * S_T \tag{4}$$

It is important to note that the multiplier is set to $S_T = 1$ for clean surfaces (i.e., based on Eq. (3)) and $S_T = 2.3$ initially attempted for all treated surfaces, which were shown earlier to be associated with higher T_{min} values compared to clean surfaces. Additionally, given the small number of data points for treated surfaces, a single value for S_T was initially attempted in Eq. (4) across all coated and oxidized surfaces. But, while the limited oxidized surface data lack obvious trends, the trends for coated surface data are both clearer and more physically sound, wherein S_T shows a positive trend with increasing thickness δ of coating, and an inverse trend relative to both thermal conductivity k_c of coating material and orientation angle θ of the heated surface. Further regression analysis helped correlate the dependence of S_T on δ (expressed in m), k_c (expressed in W.m^{-1}.K^{-1}), and θ (expressed in degrees), according to:

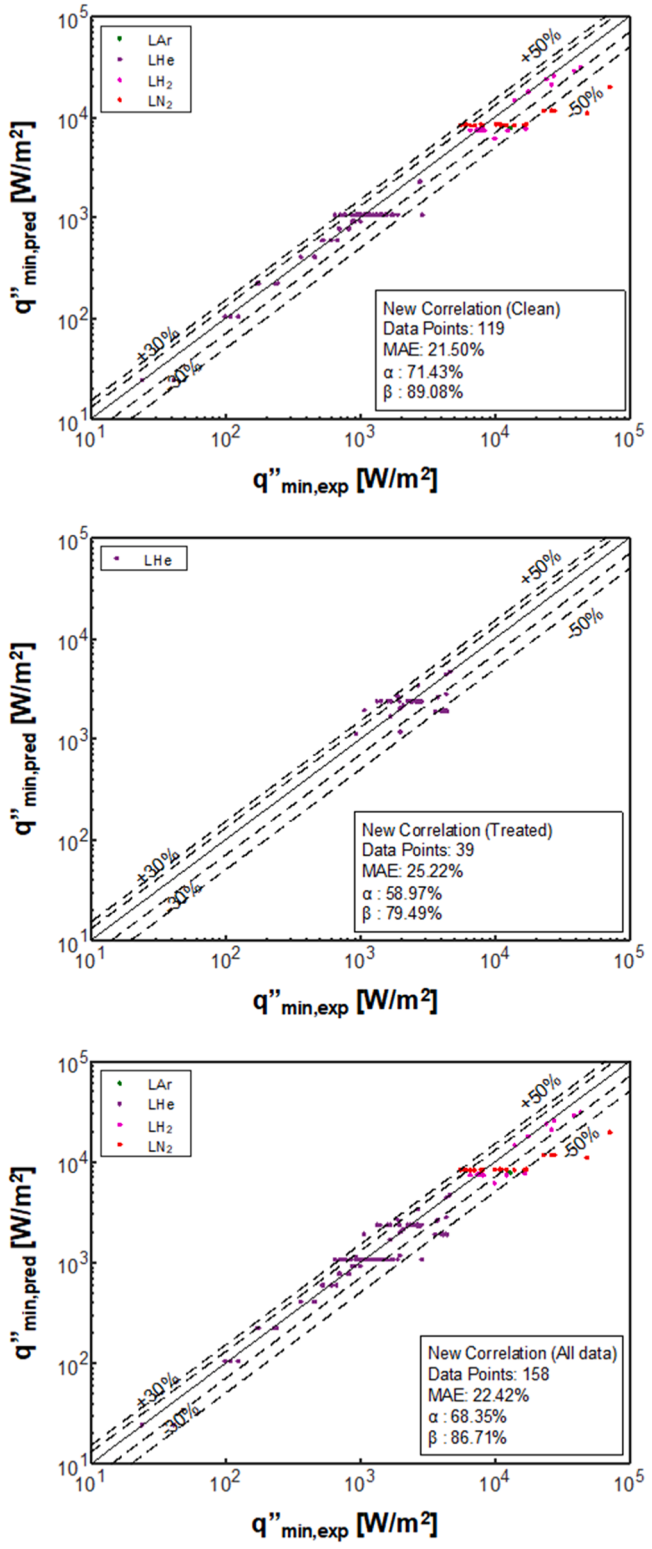

Fig. 19. Assessment of predictive accuracy of the new q"$_{min}$ correlation against data for clean surfaces, treated surfaces, and all surfaces combined.

$$S_T = \frac{\left(\delta - 1.2999 \times 10^{-6}\right)^{0.042}}{(0.06k_c)^{0.247}(\theta + 0.2)^{0.012}} \tag{5}$$

where δ is expressed in m and as summarized in Table 7, S_T= 1 for clean surfaces, S_T= 2.3 for oxidized, and its value is determined using Eq. (5) for coated. As shown in Fig. 17(a), the new correlation exhibits a remarkably low MAE of 9.05 % for clean surfaces, greatly outperforming performances of all prior correlations, Fig. 6. Moreover, effectiveness of the new correlation extends beyond clean surfaces, demonstrating exceptional performance for treated surfaces, evidenced by an impressive MAE of only 7.7 %, as shown in Fig. 17(b). Here too, by comparing Figs. 17(b) to 7, the new correlation is proven to greatly outperform all prior correlations. To provide a holistic evaluation of the new correlation's performance, Fig. 17(c) merges data for both clean and treated surfaces. Here, the new correlation shows a remarkable MAE of 8.73 % across a total of 165 data points, with 100 % of predictions falling within ±50 % of the data, and 89.7 % within ±30 %.

The performance of the new correlation for individual cryogens is provided in Fig. 18, which shows MAEs of 8.26 %, 0.1 %, 8.21 %, and 14.03 % for LHe, LAr, LN_2, and LH_2, respectively, demonstrating the "universality" of the correlation across different cryogens.

However, it's important to acknowledge that continued improvements and refinements may be warranted as more data becomes available, addressing the identified gaps highlighted in the preceding section.

5.5. New universal correlation for q"$_{min}$

Development of a new correlation for q"$_{min}$ follows a process similar to that discussed in the preceding section for T_{min} correlation. Therefore, this section will primarily focus on the outcomes of the q"$_{min}$ correlation rather than its formulation. Upon scrutinizing the results of previous q"$_{min}$ correlations in Fig. 9, it became apparent that despite slightly higher MAE of Kalinin's et al.'s [31] than those of the two best performing correlations, formulation of the new correlation is based on Kalinin's et al.'s given its effectiveness at (i) accounting for both saturation temperature and thermal properties of both heating surface and fluid, and (ii) accurately capturing T_{min} data trends. Initially, the new correlation was crafted for data pertaining to clean surfaces, after which adjustments were made for oxidized and coated surfaces through incorporation of a multiplier. The resulting correlation is expressed as:

$$q''_{min} = 0.043\left[\frac{c_{p,g}k_g^2}{\mu_g}\rho_g g(\rho_f - \rho_g)\right]^{0.567}\left(-0.107 + 0.38\,(\Delta T_{min})^{0.39}\right)^{3.094} S_q \tag{6}$$

where S_q is a multiplier intended to account for different surface conditions, and ΔT_{min} is the wall superheat at the MHF point, which is calculated using Eq. (3),

$$\Delta T_{min} = (T_c - T_{sat})\left(-9.1 + 12\left(\frac{k_f\rho_f c_{p,f}}{k_w\rho_w c_{p,w}}\right)^{0.025}\right) \tag{7}$$

As detailed in Table 7, the value of heat flux multiplier is set to S_q= 1 for clean surfaces, S_q= 2.18 for oxidized, and correlated via regression analysis for coated surfaces according to the following relation:

$$S_q = \frac{\left(\delta - 1.28 \times 10^{-6}\right)^{0.1}}{(0.132k_c)^{0.43}(\theta + 0.05)^{0.07}} \tag{8}$$

where δ is expressed in m.

Fig. 19 shows predictive accuracy of the new correlation against data for clean surfaces, treated surfaces, and all surfaces combined. Notably, the new correlation is shown achieving MAE values of 21.5 % for clean surfaces data, 25.22 % for treated, and 22.42 % for combined clean and treated. While these values are higher than corresponding T_{min} correlation's MAEs, lesser accuracy in relation to the q"$_{min}$ data, as discussed earlier, is rooted to greater discrepancies in available experimental q"$_{min}$ data compared to the T_{min} data. Nonetheless, the MAE for the new q"$_{min}$ correlation is far smaller than those of all prior correlation, which yielded MAEs above 57.67 %, 31.12 %, and 61.60 % for clean, treated, and combined surfaces.

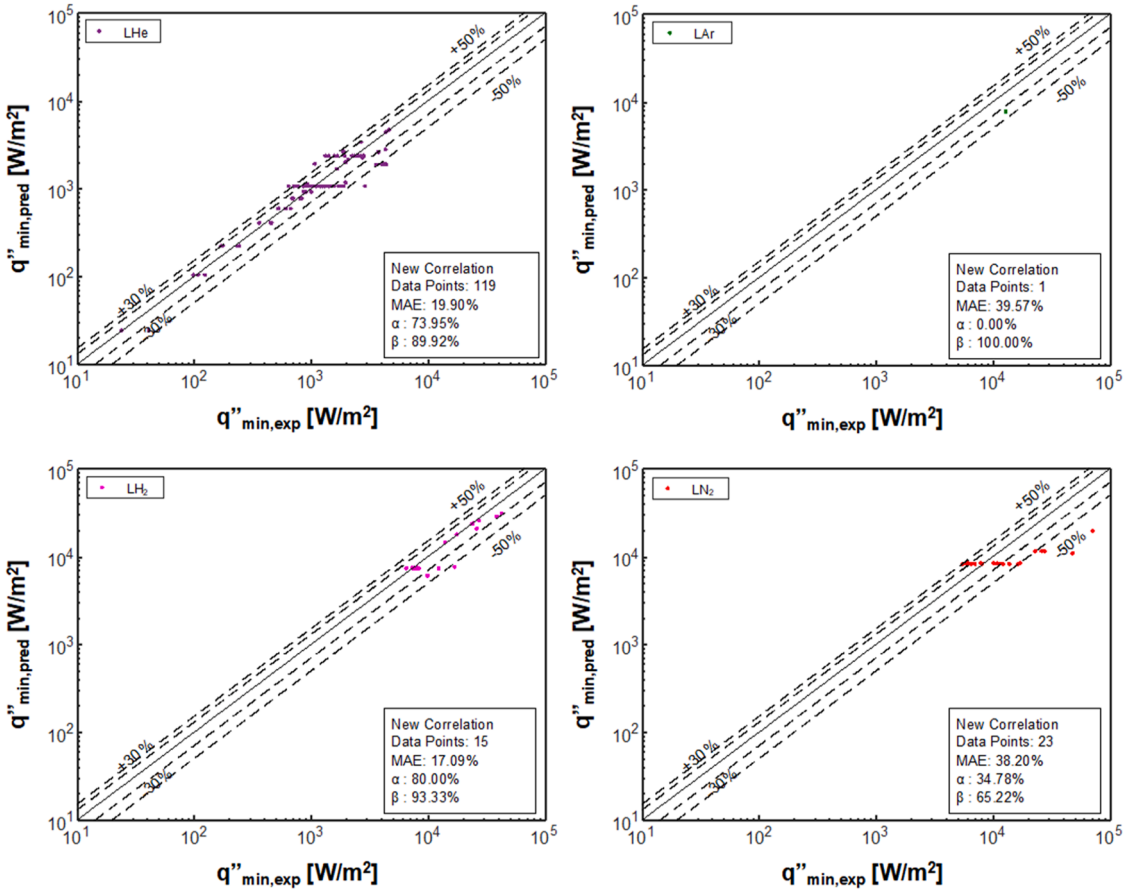

Fig. 20. Assessment of predictive accuracy of the new q''_{min} correlation against data for individual cryogens.

The performance of the new correlation for individual cryogens is provided in Fig. 20, which shows MAEs of 19.9 %, 39.57 %, 17.09 %, and 38.20 % for LHe, LAr, LN_2, and LH_2, respectively.

In closing it must be emphasized that cryogenic databases are in dire need for additional experimental work to fill the data gaps highlighted earlier. Once data is available for all cryogens of interest and over broad ranges of all relevant influencing parameters, it will be possible to explore the use of machine learning methods to correlate both T_{min} and q''_{min} data. Such methods have recently shown tremendous successes in predicting data for both flow boiling [62–64] and flow condensation [65].

6. Conclusions

This study was motivated by absence of an accurate method for predicting the minimum heat flux (MHF) point for cryogenic pool boiling. A primary reason for this deficiency is extreme sparsity of cryogenic MHF data. A broad database for multiple cryogens and which covers broad ranges of all influencing parameters is essential to formulating accurate predictive tools. The present study amassed from available literature across the globe MHF data for saturated pool boiling of cryogenic fluids from flat surfaces. The resulting Consolidated Database was used to both assess predictive accuracy of prior correlations and provided a basis for formulating new superior correlations. Following are key findings from this study.

1. A comprehensive literature review was undertaken to explore how different factors and parameters influence MHF. Additionally, a total of 9 correlations for minimum film boiling temperature (T_{min}) and 10 correlations for minimum heat flux (q''_{min}) were gathered from the literature.
2. Following the application of rigorous data rejection criteria, a meticulous selection process led to the aggregation of 165 data points for T_{min} and 158 data points for q''_{min}, collectively forming the new Consolidated Database for MHF, which encompasses four cryogens: LHe, LAr, LH_2, and LN_2. In addition to data for clean surfaces (122 points), the Consolidated Database includes data for both coated surfaces (19 points) and oxidized surfaces (20 points).
3. The accuracy of all prior correlations for T_{min} and q''_{min} was thoroughly assessed by comparing predictions against the Consolidated Database. While vast majority of these correlations yielded unacceptably high MAE values, a correlation by Kalinin et al. [31] both yielded comparatively favorable predictions for clean surfaces and successfully accounted for vitally important influences (e.g., saturation temperature and thermophysical properties of both heating surface and fluid) which were missed by most other investigators.
4. Using the Consolidated Database and leveraging insights gained from prior correlation results, especially that of Kalinin et al., new correlations for both T_{min} and q''_{min} were formulated. These new correlations were shown to provide far superior predictive accuracy compared to all prior correlations. Specifically, the new correlation for T_{min} achieved remarkable MAEs of 9.05 % for clean surfaces, 7.7 % for treated surfaces, and 8.73 % for all surfaces combined. Similarly, the new correlation for q''_{min} demonstrated MAEs of 21.50 % for clean surfaces, 25.22 % for treated surfaces, and 22.42 % for all surfaces combined.
5. Analyzing the parametric distributions within the Consolidated Database and assessing the spread of MHF values highlighted several data gaps, which were identified as paramount deficiencies to be tackled in future experimental endeavors in pursuit of any further refinement of the new correlations.

Author declaration

We wish to confirm that there are no known conflicts of interest associated with this publication and there has been no significant financial support for this work that could have influenced its outcome.

We confirm that the manuscript has been read and approved by all named authors and that there are no other persons who satisfied the criteria for authorship but are not listed. We further confirm that the order of authors listed in the manuscript has been approved by all of us.

We confirm that we have given due consideration to the protection of intellectual property associated with this work and that there are no impediments to publication, including the timing of publication, with respect to intellectual property. In so doing we confirm that we have followed the regulations of our institutions concerning intellectual property.

We understand that the Corresponding Author is the sole contact for the Editorial process (including Editorial Manager and direct communications with the office). He/she is responsible for communicating with the other authors about progress, submissions of revisions and final approval of proofs. We confirm that we have provided a current, correct email address which is accessible by the Corresponding Author and which has been configured to accept email from mudawar@ecn.purdue.edu

CRediT authorship contribution statement

Faraz Ahmad: Writing – review & editing, Writing – original draft, Validation, Software, Methodology, Investigation, Formal analysis, Data curation, Conceptualization. **Michael Meyer:** Writing – review & editing, Supervision, Resources, Project administration, Investigation, Funding acquisition. **Jason Hartwig:** Writing – review & editing, Supervision, Resources, Project administration, Methodology, Investigation, Funding acquisition, Conceptualization. **Issam Mudawar:** Writing – review & editing, Writing – original draft, Validation, Supervision, Resources, Project administration, Methodology, Investigation, Funding acquisition, Formal analysis, Conceptualization.

Declaration of competing interest

The authors declare the following financial interests/personal relationships which may be considered as potential competing interests: Issam Mudawar reports financial support was provided by NASA. Jason Hartwig reports a relationship with NASA Glenn Research Center that includes: employment. If there are other authors, they declare that they have no known competing financial interests or personal relationships that could have appeared to influence the work reported in this paper.

Data availability

The data that has been used is confidential.

Acknowledgment

The authors are grateful for financial support of the National Aeronautics and Space Administration (NASA) Small Business Technology Transfer (STTR) program under a subcontract from MTS Inc. Phase II contract 80NSSC23CA009. We also thank the Fulbright Program for providing a scholarship for the first author.

References

[1] E.W. Lemmon, I.H. Bell, M.L. Huber, M.O. McLinden, NIST standard reference database 23: reference fluid thermodynamic and transport properties-REFPROP, Version 10.0, National Institute of Standards and Technology, Gaithersburg (2018).
[2] V. Ganesan, R. Patel, J. Hartwig, I. Mudawar, Review of databases and correlations for saturated flow boiling heat transfer coefficient for cryogens in uniformly heated tubes, and development of new consolidated database and universal correlations, Int. J. Heat. Mass Transf. 179 (2021) 121656.
[3] T.J. LaClair, I. Mudawar, Thermal transients in a capillary evaporator prior to the initiation of boiling, Int. J. Heat. Mass Transf. 43 (2000) 3937–3952.
[4] G. Liang, I. Mudawar, Pool boiling critical heat flux (CHF) – part 2: assessment of models and correlations, Int. J. Heat. Mass Transf. 117 (2018) 1368–1383.
[5] I. Mudawar, R.A. Houpt, Mass and momentum transport in smooth falling liquid films laminarized at relatively high Reynolds numbers, Int. J. Heat. Mass Transf. 36 (1993) 3437–3448.
[6] C.O. Gersey, I. Mudawar, Effects of heater length and orientation on the trigger mechanism for near-saturated flow boiling critical heat flux - II. Critical heat flux model, Int. J. Heat. Mass Transf. 38 (1995) 643–654.
[7] S. Mukherjee, I. Mudawar, Pumpless loop for narrow channel and micro-channel boiling from vertical surfaces, J. Electron. Packag. 125 (2003) 431–441.
[8] M.E. Johns, I. Mudawar, An ultra-high power two-phase jet-impingement avionic clamshell module, J. Electron. Packag. 118 (1996) 264–270.
[9] W.P. Klinzing, J.C. Rozzi, I. Mudawar, Film and transition boiling correlations for quenching of hot surfaces with water sprays, J. Heat Treat. 9 (1992) 91–103.
[10] M.K. Sung, I. Mudawar, Single-phase and two-phase heat transfer characteristics of low temperature hybrid micro-channel/micro-jet impingement cooling module, Int. J. Heat. Mass Transf. 51 (2008) 3882–3895.
[11] M.K. Sung, I. Mudawar, Single-phase and two-phase hybrid cooling scheme for high-heat-flux thermal management of defense electronics, J. Electron. Packag. 131 (2009) 021013.
[12] C. Cai, I. Mudawar, H. Liu, Mechanistic method to predicting minimum heat flux point wall temperature in saturated pool boiling, Int. J. Heat. Mass Transf. 156 (2020) 119854.
[13] A. Sakurai, M. Shiotsu, K. Hata, Effect of system pressure on film-boiling heat transfer, minimum heat flux, and minimum temperature, Nucl. Sci. Eng. 88 (1984) 321–330.
[14] S.M. Kozlov, S.V. Nozdrin, Heat transfer and boundaries of its regimes during hydrogen boiling at different metallic surfaces, Cryogenics 32 (1992) 245–248.
[15] V.I. Deev, V.E. Keilin, I.A. Kovalev, A.K. Kondratenko, V.I. Petrovichev, Nucleate and film pool boiling heat transfer to saturated liquid helium, Cryogenics 17 (1977) 557–562.
[16] L. Bewilogua, R. Knöner, H. Vinzelberg, Heat transfer in cryogenic liquids under pressure, Cryogenics 15 (1975) 121–125.
[17] A.P. Butler, G.B. James, B.J. Maddock, W.T. Norris, Improved pool boiling heat transfer to helium from treated surfaces and its application to superconducting magnets, Int. J. Heat. Mass Transf. 13 (1970) 105–115.
[18] D.N. Lyon, Boiling heat transfer and peak nucleate boiling fluxes in saturated liquid helium between the lamda and critical temperatures, Adv. Cryog. Eng. 10 (1965) 371.
[19] V.E. Keilin, E.Y. Klimenko, V.H. Shleifman, Inzhenernofizicheskij zhurnal, XXIY 3 (1973) 425.
[20] V.A. Grigoriev, V.V. Klimenko, Y.M. Pavlo, Y.V. Ametistov, A.V. Klimenko, Characteristic curve of helium pool boiling, Cryogenics 17 (1977) 155–156.
[21] H. Ogata, H. Mori, Steady state heat transfer in transition boiling of helium on copper surfaces, Cryogenics 33 (1993) 640–642.
[22] G.R. Chandratilleke, S. Nishio, H. Ohkubo, Pool boiling heat transfer to saturated liquid helium from coated surface, Cryogenics 29 (1989) 588–592.
[23] A. Iwamoto, T. Mito, K. Takahata, N. Yanagi, J. Yamamoto, Heat transfer from an oxidized large copper surface to liquid helium: dependence on surface orientation and treatment, Adv. Cryog. Eng. (1996) 217–224.
[24] R. Patel, M. Meyer, J. Hartwig, I. Mudawar, Review of cryogenic pool boiling critical heat flux databases, assessment of models and correlations, and development of new universal correlations, Int. J. Heat. Mass Transf. 190 (2022) 122579.
[25] F. Ahmad, S. Kim, M. Meyer, J. Hartwig, I. Mudawar, Saturated nucleate pool boiling of cryogenic fluids: review of databases, assessment of existing models and correlations, and development of new universal correlation, Int. J. Heat. Mass Transf. 231 (2024) 125807.
[26] F. Ahmad, M. Meyer, J. Hartwig, I. Mudawar, Saturated pool film boiling of cryogenic fluids review of databases, assessment of existing models and correlations, and development of new universal correlation, Int. J. Heat. Mass Transf. (2024) in review.
[27] P. Spiegler, J. Hopenfeld, M. Silberberg, C.F. Bumpus Jr, A. Norman, Onset of stable film boiling and the foam limit, Int. J. Heat. Mass Transf. 6 (1963) 987–989.
[28] P.J. Berenson, Film-boiling heat transfer from a horizontal surface, J. Heat. Transf. 83 (1961) 351–358.
[29] K.J. Baumeister, F.F. Simon, Leidenfrost temperature—its correlation for liquid metals, cryogens, hydrocarbons, and water, J. Heat. Transfer. 95 (2) (1973) 166–173.
[30] R.E. Henry, A correlation for the minimum film boiling temperature, AIChE Symp. Ser. 138 (1974) 81–90.
[31] E.K. Kalinin, I.I. Berlin, V.V. Kostyuk, E.M. Nosova, Heat transfer in transition boiling of cryogenic liquids, Adv. Cryog. Eng. (1975) 273–277.
[32] J.H. Lienhard, Correlation for the limiting liquid superheat, Chem. Eng. Sci. 31 (1976) 847–849.
[33] D. Schroeder-Richter, G. Bartsch, The Leidenfrost phenomenon caused by a thermo-mechanical effect of transition boiling: a revisited problem of non-equilibrium thermodynamics, in: Fundamentals of phase change: boiling and condensation, ASME-HTD, New York, 1990, pp. 13–20.
[34] E. Aursand, S.H. Davis, T. Ytrehus, Thermocapillary instability as a mechanism for film boiling collapse, J. Fluid. Mech. 852 (2018) 283–312.

[35] S.S. Kutateladze, Heat Transfer in Condensation and Boiling, US Atomic Energy Commission, Technical Information Service, 1959.
[36] N. Zuber, Hydrodynamic aspects of boiling heat transfer, US Atomic Energy Commiss., Tech. Inf. Serv. (1959).
[37] V.G. Morozov, An experimental investigation of the cessation of film boiling of a liquid on a submerged heating surface, Int. Chem. Eng. 3 (1963) 48–51.
[38] A. Padilla, Film Boiling of Potassium on a Horizontal Plate, doctoral thesis, University of Michigan, USA, 1966.
[39] R.C. Kesselring, P.H. Rosche, S.G. Bankoff, Transition and film boiling from horizontal strips, AIChe J. 13 (1967) 669–675.
[40] J.H. Lienhard, V.K. Dhir, On the prediction of the minimum pool boiling heat flux, J. Heat Transf. 102 (1980) 457–460.
[41] M. Shoji, H. Nagano, Minimum heat flux of saturated pool boiling on a horizontal heated surface, Tran. JSME Ser. B 52 (1987) 2431–2436.
[42] V.V. Klimenko, Film boiling on a horizontal plate—new correlation, Int. J. Heat. Mass Transf. 24 (1981) 69–79.
[43] A. Rohatgi, WebPlotDigitizer 2018, https://automeris.io.
[44] C.R. Class, J.R. DeHaan, M. Piccone, R.B. Cost, Boiling heat transfer to liquid hydrogen from flat surfaces, in: Proc. 1959 Cryogenic Engineering Conf., University of California, Berkeley, Springer, 1960, pp. 254–261.
[45] P.C. Wayner Jr, S.G. Bankoff, Film boiling of nitrogen with suction on an electrically heated porous plate, AIChe J. 11 (1965) 59–64.
[46] R.D. Cummings, J.L. Smith, Boiling Heat Transfer to Liquid Helium, Pergamon Press, Oxford, (1966) 85-95.
[47] J.A. Clark, E.W. Lewis, H. Merte Jr, Boiling of Liquid Nitrogen in Reduced Gravity Fields with Subcooling, Heat Transfer Lab, Dept. of Mech. Eng., Univ. of Michigan, 1967.
[48] C.E. Price, Film Boiling from Inclined Flat Surfaces (1969), Masters thesis, U. Missouri-Rolla, 1969.
[49] H. Merte Jr, J.A. Clark, Boiling heat transfer with cryogenic fluids at standard, fractional, and near-zero gravity, J. Heat Transf. 86 (1964) 351–358.
[50] H.J. Sauer Jr, K.M. Ragsdell, Film pool boiling of nitrogen from flat surfaces, in: Proc. 1970 Cryogenic Eng. Conf., University of Colorado, Springer, Boulder, Co, 1971, pp. 412–415.
[51] M. Jergel, R. Stevenson, Contribution to the static heat transfer to boiling liquid helium, Cryogenics 14 (1974) 431–433.
[52] J.L. Swanson, H.F. Bowman, Transient surface temperature behavior in nucleate pool-boiling nitrogen, Proc. 5th Int. Heat Transfer Conf., Tokyo, Japan, 1974.
[53] H. Ogata, W. Nakayama, Heat transfer to subcritical and supercritical helium in centrifugal acceleration fields 1. Free convection regime and boiling regime, Cryogenics 17 (1977) 461–470.
[54] H. Ogata, Heat transfer to boiling helium from machined and chemically treated copper surfaces, Adv. Cryog. Eng. 27 (1981) 309–317.
[55] V.V. Klimenko, A.G. Shelepen, Film boiling on a horizontal plate—a supplementary communication, Int. J. Heat. Mass Transf. 25 (1982) 1611–1613.
[56] M.W. Scheiwe, U. Hartmann, Heat transfer from warm plates of cryobiologic interest to liquid nitrogen, in: Proc. 9th Int. Cryogenic Eng. Conf., Elsevier, Kobe, Japan, 1982, pp. 81–84.
[57] S. Nishio, Study on minimum heat-flux point during boiling heat transfer on horizontal plates, Trans. Jpn. Soc. Mech. Eng.-B 51 (1985) 582–590.
[58] S. Nishio, G.R. Chandratilleke, Steady-state pool boiling heat transfer to saturated liquid helium at atmospheric pressure, JSME Int. J. Ser. 2 (1989) 639–645, 32.
[59] A. Iwamoto, T. Mito, K. Takahata, N. Yanagi, J. Yamamoto, Heat transfer of a large copper plate to liquid helium applicable to large scale superconductors, Cryogenics. (Guildf) 34 (1994) 321–324.
[60] A. Iwamoto, R. Maekawa, T. Mito, J. Yamamoto, Steady state heat transfer characteristics in He I with different surface area, Adv. Cryog. Eng. (1998) 1481–1487.
[61] T. Jin, J. Hong, H. Zheng, K. Tang, Z. Gan, Measurement of boiling heat transfer coefficient in liquid nitrogen bath by inverse heat conduction method, J. Zhejiang Univ. Sci.-A 10 (2009) 691–696.
[62] Y. Qiu, D. Garg, L. Zhou, C.R. Kharangate, S. Kim, I. Mudawar, An artificial neural network model to predict mini/micro-channels saturated flow boiling heat transfer coefficient based on universal consolidated data, Int. J. Heat. Mass Transf. 149 (2020) 119211.
[63] Y. Qiu, D. Garg, S. Kim, I. Mudawar, C.R. Kharangate, Machine learning algorithms to predict flow boiling pressure drop in mini/micro-channels based on universal consolidated data, Int. J. Heat. Mass Transf. 178 (2021) 121607.
[64] I. Mudawar, S.J. Darges, V.S. Devahdhanush, Prediction technique for flow boiling heat transfer and critical heat flux in both microgravity and earth gravity via artificial neural networks (ANNs), Int. J. Heat. Mass Transf. 220 (2024) 124998.
[65] L. Zhou, D. Garg, Y. Qiu, C.R. Kharangate, S. Kim, I. Mudawar, Machine learning algorithms to predict flow condensation heat transfer coefficient in mini/micro-channel utilizing universal data, Int. J. Heat. Mass Transf. 162 (2020) 120351.